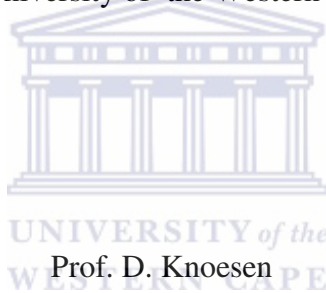


Synthesis and Characterisation of ^{114}Cd targets

Ntombizonke Yvonne Kheswa

Thesis presented in fulfillment of the requirements for the degree of Master of Sciences in the Department of Physics at the University of the Western Cape.



Supervisors:

Prof. D. Knoesen

Department of Physics

University of the Western Cape

Dr. M. Topic

Material Research Department

iThemba LABS

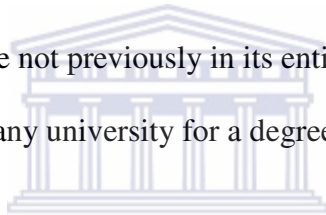
November 2011




UNIVERSITY *of the*
WESTERN CAPE

DECLARATION

I, the undersigned, hereby declare that the work contained in this thesis is my own original work and that I have not previously in its entirety or in part submitted it at any university for a degree.



UNIVERSITY *of the*
WESTERN CAPE

Signature: 

Date:20 July 2012.....

ABSTRACT

Synthesis and Characterisation of ^{114}Cd targets

To study nuclear reactions and nuclear structures, target materials are bombarded with high-energy particles. The target material can either be in a form of a metal film or gas. A target material designed to study certain nuclear reactions or to produce nuclei to study their structure should yield as minimum as possible of competing reactions under ion bombardment. This requires a chemically and isotopically pure target material prepared as a self supporting thin film, or as alternative, prepared on a thin carrier foil. Additional requirement for lifetime measurement experiments are homogeneity and precise thickness of the target material. Some of the data obtained from the stopping power experiment where targets of ^{114}Cd were used for lifetime measurement are presented. Moreover, a nuclear target should influence the spectroscopic resolution as little as possible. Thus, film thickness must be adjusted to the respective reaction under study while observing the optimum thickness homogeneity.

Metal films of ^{114}Cd with different thicknesses were synthesised by vacuum evaporation and rolling techniques. These films were used as target materials in a nuclear physics experiment conducted at iThemba LABS. The title of the experiment was “the investigation of lifetime measurements of dipole band in ^{136}Nd and ^{137}Nd with AFRican Omnipurpose Detector for Innovative Techniques and Experiment (AFRODITE) using Doppler Shift Attenuation Method (DSAM)”. During the experiments, these targets were bombarded with a ^{28}Si beam with energy of 155 MeV. Material characterisation of synthesised ^{114}Cd targets was conducted to determine if changes occurred on the material when irradiated with the beam. The characterisations of target materials were performed before they were used in an experiment and after.

For surface topography and morphology of the targets under investigation, atomic force microscopy (AFM) and scanning electron microscopy (SEM) technologies were

employed. Possible microstructure changes were investigated by optical microscopy at the nuclear microprobe facility at iThemba LABS. The techniques employed were Rutherford backscattering spectroscopy (RBS) and Particle Induced X-ray Emission (PIXE). These methods were for determination of the target thickness (before and after being exposure to radiation condition) and elemental distribution in a target. The phase analysis of target materials was performed by X-ray diffraction method. All the findings showed no defects on the targets caused by the high energy beam. The target thickness remained unchanged on the entire surface area including the area in the target where the beam of ^{28}Si was focused on (beam spot).



KEYWORDS

- Nuclear Targets
- Target Thickness
- Characterization
- Rutherford Backscattering
- Particle Induced X-ray Emission
- X-ray Diffraction
- Atomic Force Microscopy
- Scanning Electron Microscopy
- Rolling Method
- Vacuum Deposition



ACKNOWLEDGEMENTS

I would like to express my heartfelt gratitude to Almighty God for the divine strength, hope and courage He gave me throughout this study and the following:

- To Prof. Dirk Knoesen my supervisor for all the supervision, academic support and all the recommendations he gave during the cause of this work.
- I extend my thanks to my co-supervisor Dr Mira Topic for her patience, honesty, motivation, guidance and instructions that assisted to the fulfillment of this work.
- iThemba LABS for awarding me financial assistance toward studying and believing in me.
- National Research Foundation for financial assistance provided during the course of study.
- I would like to express my sincere gratitude to my friends and colleagues Prof. Rainer and Dr Evgenia Lieder. Prof. Lieder for being available at all times in reading my work and give recommendations, that was a big contribution in this study. You were both with me in the beginning of this work till the end. Your endless support gave me hope, strength and encouragement.
- My sincere thanks go to my colleague Dr Peane Maleka for all the assistance, advices and support he gave. Availing yourself at all times to read at my work inspite of your other commitments. You played an important role during the course of this work. “Umuntu Ngumuntu Ngabantu”.
- Dr Obed Shirinda and Dr Sifiso Ntshangase you have made it sure that the final work submitted is in good order and presentable, I am humbly thanking you both for that. Ngithi kini nobabili Ubuntu mabande.
- My appreciation goes to my colleagues in the Department of nuclear Physics of iThemba LABS, Dr Elena Lawrie and Dr Retief Neveling for their willingness support and help for me to be able to begin this work.
- To the following staff at Materials Research Department (iThemba LABS):
- Prof. Carlos Pieneda, Phillip Sechogela for their help during RBS and PIXE analysis.
- Mr Zakhele Khumalo for help during XRD analysis.
- Dr. Mlungisi Nkosi for AFM analysis.

- I would like to express my huge thanks to my parents and siblings for their encouragements and prayers. You should know that this is what kept me going and looking forward to finishing.
- Last but not least, a big thank you to my family for your patience, love, support and motivation you gave me since I started studying. Nqobile my baby girl, I thank you for your understanding that mummy was also studying.



CONTENTS

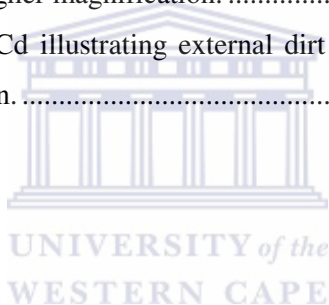
CHAPTER 1 BACKGROUND.....	1
1.1 Introduction.....	1
1.2 Requirements for nuclear targets	2
1.3 Scope of the investigation.....	3
CHAPTER 2 LITERATURE REVIEW.....	5
2.1 Methods for isotope separation	5
2.1.1 Diffusion process for isotope separation	5
2.1.2 Isotope separation by gas centrifuge method.....	7
2.1.3 Electromagnetic isotope separation method.....	8
2.1.4 Laser isotope separation method.....	9
2.2 Targets and nuclear physics experiments	11
2.2.1 Characteristics of cadmium and other isotopically enriched targets	13
2.2.2 Nuclear physics experiments and their respective target requirements.....	14
2.3 Techniques for targets manufacturing.....	15
2.3.1 Multiple painting method.....	16
2.3.2 Depositions methods	16
2.3.3 Vacuum evaporation technique.....	17
2.4 Techniques used in target characterisation	19
CHAPTER 3 MATERIALS AND METHODS.....	22

3.1	Manufacturing of targets	22
3.1.1	Rolling of metallic ¹¹⁴ Cd	25
3.1.2	Application of ¹¹⁴ Cd targets	26
3.2	Characterisation of ¹¹⁴Cd targets	29
3.2.1	Rutherford backscattering (RBS).....	29
3.2.2	Particle induced X-ray emission (PIXE)	32
3.2.3	Surface characterization by atomic force microscope (AFM).....	33
3.2.4	X-ray diffraction analysis (XRD)	35
3.2.5	Scanning electron microscopy (SEM)	38
3.3	Conclusion	41
<i>CHAPTER 4 RESULTS AND DISCUSSION</i>		<i>42</i>
4.1	Target manufacturing	42
4.2	Nuclear microprobe results	43
4.2.1	Thickness determination and quantification by RBS	43
4.2.2	Elemental distribution analysis of by PIXE.....	45
4.2.3	Phase analysis by X – ray diffraction (XRD)	46
4.2.4	Surface topography and morphology characterisation	48
4.2.4.1	Atomic force microscopy (AFM)	48
4.2.4.2	Scanning electron microscopy (SEM)	50
4.3	Conclusion	52
<i>CHAPTER 5 SUMMARY</i>		<i>54</i>
<i>REFERENCES.....</i>		<i>55</i>

LIST OF FIGURES

Figure 2.1: The schematic showing the isotope separation by diffusion process [Set09].	6
Figure 2.2: (a) Cascades of gas centrifuge for isotope separation arranged in series and parallel positions and (b) schematic drawing of a gas centrifuge [Wat03][Wiki].	8
Figure 2.3: The schematic drawing showing various components of the calutron mass spectrometer for electromagnetic isotope separation process [Smi11].	9
Figure 2.4: (a) A schematic drawings showing a general isotope separation by laser and (b) Atomic Vapour Laser Isotope Separation (AVLIS) process [Mai93][Fei93].	11
Figure 2.5: SEM images of Bi targets showing the morphology (a) before and (b) after being destroyed by the heavy ion beam. The surface topographic graphs are from the bright scan lines [Mun88].	12
Figure 2.6: These are two pictures of typical electroplating cells. The plating cell on the left is for vertical plating and on the right is the modified design which uses horizontal plating type [Ebe04][Lie08].	17
Figure 2.7: The RBS spectra of Silicon target (a) contaminated with copper and (b) free from copper contamination [Mee93].	21
Figure 3.1: Schematic drawing of a resistive heating vacuum evaporator used to deposit ^{114}Cd .	24
Figure 3.2: A schematic diagram illustrating a rolling process [Gro99].	25
Figure 3.3: Polished stainless steel plates of an envelope type showing, from right to left, the shape deformation after several strikethrough in mills.	26
Figure 3.4: Schematic diagram of the AFRODITE instrument (left) and the image (right) showing the target chamber, clover detectors and the beam line.	28
Figure 3.5: Two Cadmium targets with beam spots produced after irradiation with ^{28}Si beam. Targets were produced by vacuum deposition and rolling.	29
Figure 3.6: A schematic representation of a Rutherford backscattering process at a sample surface [Woo84].	30
Figure 3.7: AFM schematic drawing of iThemba LABS showing sample surface, cantilever and tip, photodiodes, laser and detector.	35
Figure 3.8: The schematic drawing of different sets of crystallographic planes that occur according to the Bragg's condition [Hun08].	37
Figure 3.9: An image of D8 Advance Bruker X-ray diffractometer employed during the analysis of the targets.	38

Figure 3.10: The schematic diagram showing general operational components of the SEM instrument used during the analysis of ^{114}Cd target at the University of Western Cape.....	40
Figure 4.1: The RBS spectrum of ^{114}Cd target before being irradiated with ^{28}Si projectile.....	44
Figure 4.2: RBS spectrum of ^{114}Cd obtained on the beam spot resulted after the experiment.	45
Figure 4.3: The contour maps of 3.6 mg.cm^{-2} obtained using the (a) L lines and (b) K lines during PIXE analysis.	46
Figure 4.4: The XRD spectra of two ^{114}Cd targets.	47
Figure 4.5: (a) AFM images representing a three dimensional images of unirradiated 3.6 mg.cm^{-2} target taken using different surface areas and (b) A three dimensional AFM image taken on beam spot of a 3.6 mg.cm^{-2} ^{114}Cd target.	49
Figure 4.6: Surface morphology obtained by SEM of a 12.6 mg.cm^{-2} ^{114}Cd target using a 35x magnification.	50
Figure 4.7: SEM images of ^{114}Cd target with a thickness of 12.6 mg.cm^{-2} obtained using lower (a) and (b) higher magnification.	51
Figure 4.8: SEM images of ^{114}Cd illustrating external dirt from the target surface taken at higher magnification.	52



LIST OF TABLES

Table 4.1: List of six ^{114}Cd targets, produced by vacuum evaporation as well as rolling techniques, and their thicknesses based on mass and area measurement.42



CHAPTER 1 BACKGROUND

This chapter gives a highlight of the nuclear physics research conducted at iThemba LABS and instrumentation used. The chapter is divided into three sections, where the purpose of the research is described in section 1.1, section 1.2 describes nuclear targets and their requirements for nuclear physics experiments and section 1.3 is the scope of the investigation of the study.

1.1 Introduction

The main aim of this work was to synthesise and characterise ^{114}Cd targets for an accelerator experiment at iThemba LABS on investigation of lifetimes of dipole bands in $^{136,137}\text{Nd}$ with AFRODITE using DSAM. During the experiment, targets were bombarded with ^{28}Si projectiles. Targets needed are self-supporting films of uniform thickness. In this type of experiment, the target is chosen such that it partially slows down the recoils in the target and then escape into vacuum [Lie09]. Therefore, three targets with different thicknesses were requested for the experiment to investigate which one would yield better results. The targets thicknesses were categorised as thin (0.5 mg.cm^{-2}), semi-thick ($3.6 - 4 \text{ mg.cm}^{-2}$) and thick (7 mg.cm^{-2}). Presently, the type of experiments performed at iThemba LABS are in the fields of nuclear reaction, nuclear structure and in application such as neutron physics and environmental studies.

There are three types of instruments dedicated to facilitate nuclear physics research at iThemba LABS and they are: (i) AFRican Omnipurpose Detector for Innovative Techniques and Experiment (AFRODITE) – a 4π γ -ray detector array, (ii) K600 magnetic spectrometer for high energy resolution measurements and (iii) A-line scattering chamber for the detection of light and heavy ions produced from nucleus – nucleus collisions [Khe08]. For each instrument, targets requirements depend on the experimental needs including the set-up of the experiment. In many cases target for physical or chemical research work at accelerators has to be prepared in the form of a uniform, self supporting thin film of thicknesses ranging from $0.1 \mu\text{m} - 10 \mu\text{m}$. In

nuclear physics experiments, thickness of a target is normally quoted in $\mu\text{g}\cdot\text{cm}^{-2}$ or $\text{mg}\cdot\text{cm}^{-2}$ and is referred to as target areal density. The advent of accelerators capable of producing heavy ion beams of a well defined and stable energy gave drive to the development of thin targets. Furthermore, the high-resolution solid-state detectors and low-noise electronics also increased the need for high purity thin targets, which are mostly enriched isotopes [For83a][Dio91][Chi71].

1.2 Requirements for nuclear targets

Presently, targets for nuclear physics and nuclear chemistry experiments are mostly manufactured using stable or radioactive isotopes. Isotopically enriched targets are preferred in nuclear research because they mainly provide the nuclides of interest only and these assist researchers during data analysis since there is a minimum background. The targets of single nuclides (isotope) are mostly used in studies for high-resolution nuclear spectroscopy and investigation of nuclear reactions.

In material sciences however, ion beams with mixtures of different elements are used as samples. For applications in solid state physics and studies of hyperfine interactions between crystal fields and electromagnetic properties of nuclei, single crystal samples are used [Mai81]. By definition a target may be considered as an orderly array of atoms of one or more elements intended to intercept various forms of radiation for the purpose of studying their interactions.

The purpose for desiring a homogeneous array of target atoms is somewhat important. Adding to this, specific target thicknesses are of importance in order to characterise the response of the target to heavy ion beams of certain energy, e.g. slowing down of projectiles and recoiling produced nuclei. All this depends on energies per nucleon and energy resolution [Mai81]. In general, charged particles of electromagnetic interactions with atoms are characterise by the formation of electromagnetic or particle emission from the target. Emissions of this type have definite energies and angular distributions which can be used by the researcher to observe the type of interactions which have occurred. Furthermore, energy states of orbital electrons or target nuclei from the interactions can be determined from this reaction [Mai81].

A target designed to study certain nuclear reactions or to produce nuclei to study their nuclear structure should yield as few as possible competing reactions under ion bombardment. Moreover, a target should influence the spectroscopic resolution as little as possible [Mai81][Yaf62]. This requires a chemically and isotopically pure target material prepared as a self supporting thin film, or alternatively prepared on a thin carrier foil. This is particularly important for electron and charged particle spectroscopy and high spin nuclear spectroscopy with heavy ion induced reactions to minimize Doppler broadening [Yaf62][Dio91]. In cases where Doppler – shift experiments are conducted, thick targets are required. This is necessary since their thickness should be able to stop the recoiling nuclei in the target under study. In other cases targets for the Doppler Shift Attenuation Method (DSAM) are constructed as thin deposits of the target nuclide on relatively thick supports made from heavy elements [Kob82][Gal70]. In addition, deposits must be uniform with a void free adherent bond to the support material.

Voids in the bond region can lead to inaccuracies in lifetime measurements because of broadening of the gamma ray energy peaks. Since the bulk density value is used in stopping power calculations, voids would certainly cause errors in measurements. Targets must be free from contaminants because of inherent changes in density and stopping power which these nuclides may cause. Targets are not expected to be in metallic film form all the time but gas targets made of stable or radioactive isotopes are also used. Gas targets are normally used in applications for nuclear reaction studies especially when high purity targets are needed for use in high resolution accelerators [Mai81]. During the early invention of targetry, presently as well, powder targets of specific thicknesses were also used in the applications of nuclear research [Sto97][Suz70].

1.3 Scope of the investigation

In the present study, the manufacturing and characterisation of ^{114}Cd targets is described in detail. Particular interest in this study was to investigate whether the properties of the target material (e.g. thickness) will be affected when bombarded with

the ^{28}Si projectile. This study comprises of five chapters. In chapter 2, literature review conducted for this study is presented. Chapter 3 describes the methods and the instrumentation used for the investigation. The surface topography and morphology were studied by AFM and SEM, respectively and are described in detail in chapter 3. Thickness measurements and possible microstructure changes were investigated by RBS and PIXE and the full description of the methods is given also in chapter 3. The phase analyses of target materials were performed by XRD. Chapters 4 and 5 give the results, discussion and the conclusion drawn from this study.



CHAPTER 2 LITERATURE REVIEW

This chapter is divided into four sections whereby section 2.1 describes the methods used for isotope separations. There are various methods available for the separation of isotopes of elements; in this study only four of the mostly used are discussed. In section 2.2, targets and type of nuclear physics experiments conducted are discussed. Section 2.3 and 2.4 describes methods for target manufacturing and their characterization methods.

2.1 Methods for isotope separation

Highly enriched isotopes are used in all branches of nuclear research, including physics, chemistry, material science, medicine, biology, geosciences and engineering, and their use has continued to expand [Tak07]. The isotopic enrichment and production are carried out by using four different processes, which are: diffusion, centrifugal, electromagnetic and laser enrichment and they are described below in detail [The79]. There are also other methods like electrolysis, distillation and isotope exchange which are used in isotope enrichment.

2.1.1 Diffusion process for isotope separation

Diffusion processes are classified as gaseous diffusion, diffusion in a vapour stream and thermal diffusion. In the gaseous diffusion method, a gaseous compound of an element being separated is pumped at low pressure through a porous membrane where two isotopes with the same energy but different average velocities (because of their mass difference) are separated. Lighter molecule penetrates the membrane faster than the heavier molecule since the difference in speed is proportional to the square root of the mass ratio. The method is considered expensive sometimes if the difference in molecular masses is small which requires that the process to be repeated many times [The79].

In the diffusion in a vapour stream method, the isotope separation is conducted in a cylindrical vessel which is divided vertically by a diaphragm. The diaphragm contains about 10^3 openings per cm^3 . The gaseous isotopes move against a stream of secondary vapour. Lighter molecules have a greater coefficient of diffusion than the heavier ones therefore, are enriched from the opposite side of the cylinder. A thermal diffusion method consists of two vertical concentric pipes heated to different temperatures. The mixture to be separated is introduced into the space between the heated pipes. The method relies on temperature drop between the surfaces of the pipes which generates a diffusion flux. This leads to a difference in the concentration of the isotopes in the cross section of the column. At the same time this temperature drop leads to the generation of vertical convection flows of the gas. Consequently, the lighter isotopes concentrate near the heated inner pipe and move upward. In the thermal diffusion method, gas and liquid isotopes can be separated and a variety of isotopes as compared to gaseous diffusion and diffusion in a stream vapour. Figure 2.1 is the schematic drawing highlighting the isotope separation process by diffusion.

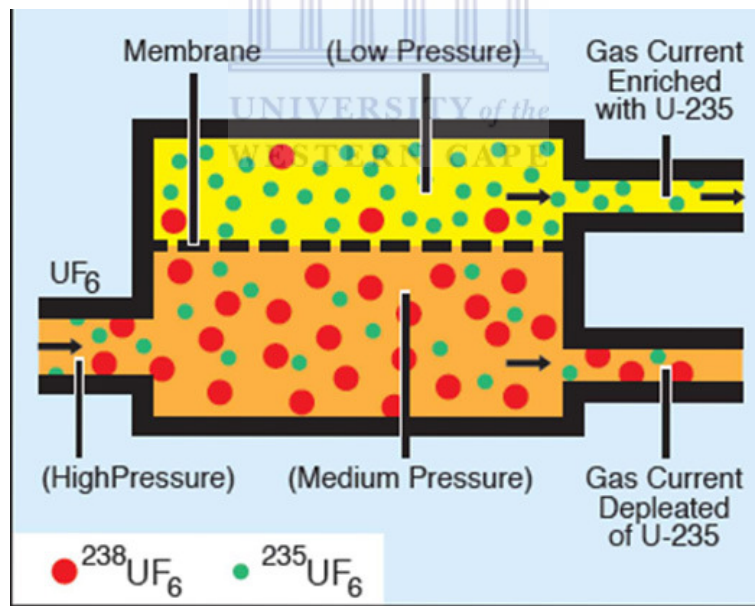


Figure 2.1: The schematic showing the isotope separation by diffusion process [Set09].

2.1.2 Isotope separation by gas centrifuge method

In the centrifugation method, the material is rotated rapidly by a centrifuge allowing heavier isotopes to move to an outer radial wall. This is done in a gaseous form using cascades of centrifuges (see figure 2.2a). This principle is the modification of the Zippe-type centrifuge which yielded a better enrichment of isotopes of uranium during the birth of isotope separation [Wat03][Bor00]. A cascade comprises of several stages of gas centrifuges connected in series and parallel in order to attain high enrichment of isotopes and also an increase in the product flow rate [Hou08]. Cascades are divided into two groups, namely enriching and stripping stages. There are three mostly used types of centrifuges which are evaporative, concurrent and countercurrent [Kar51][Hou08].

In the evaporative centrifuge a small amount of liquid is introduced into the centrifuge forming a layer at the periphery. During the spinning of the rotor, vapour is removed slowly through a shaft along the axis. In this way Rayleigh distillation of the liquid is thus obtained [Kar51][Wat03]. The concurrent centrifuge also known as the flow - through centrifuge involves gaseous flow of the continuous stream separator. As originally conceived, a single stream of gas enters one end of the rotor through a hollow shaft and the two streams are taken off the other end, one from the periphery and the other near the axis. This method produces a small change in concentration per machine.

The countercurrent flow type was designed to attain considerable separation in a single centrifuge, thus reducing the number of stages required and the amount of material circulated between stages. Countercurrent separation has the property of multiplying the equilibrium process factor many times in one unit. Since a large separation is obtained in one unit, the recycling between units is not necessary unlike in the previous method. Furthermore, the problem of cascade operation is very considerably simplified since the number of units in series required to effectuate a given fractionation decrease enormously. The cascade becomes broad instead of long and is easily broken down into independent parallel sections. Countercurrent flow is also efficient from a process standpoint because it is possible to maintain maximum

separative power through the entire unit. This method is more favoured for industrial use for the enrichment of isotopes as power consumption is greatly reduced when compared to more conventional methods such as gaseous diffusion methods [Kar51][Hou08] . An example of a gas centrifuge is shown in figure 2.2 (b).

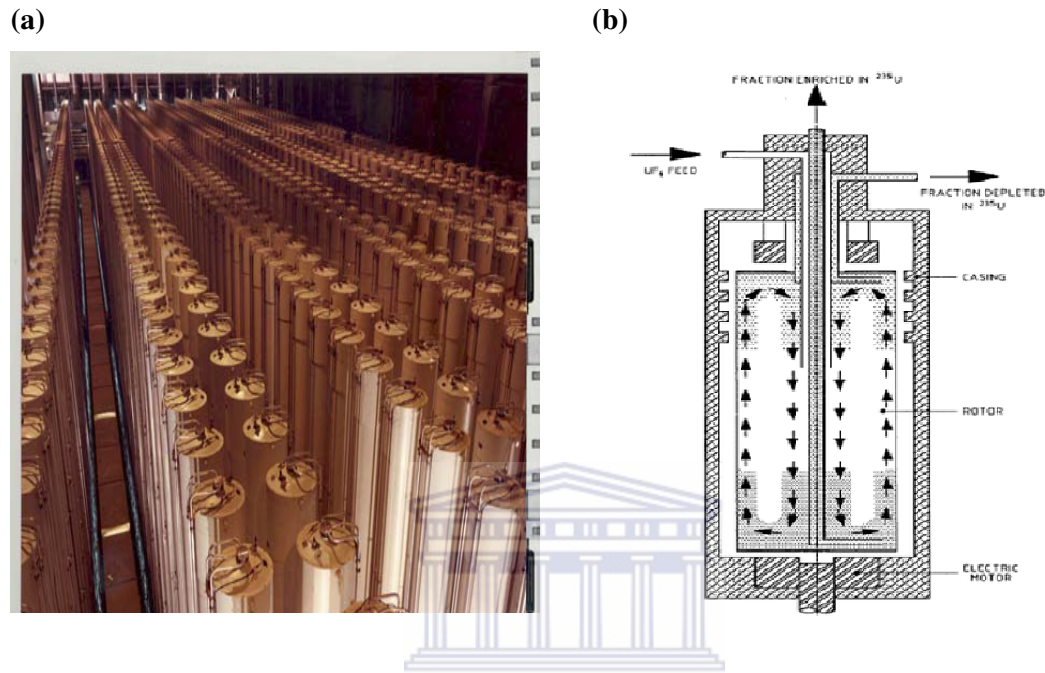


Figure 2.2: (a) Cascades of gas centrifuge for isotope separation arranged in series and parallel positions and (b) schematic drawing of a gas centrifuge [Wat03][Wiki].

2.1.3 Electromagnetic isotope separation method

Electromagnetic separation is conducted by using high current mass spectrometers which are known as calutron (see figure 2.3). The process is based on the motion of an energetic ion in a magnetic field [Tra93]. Primary components of an electromagnetic isotope separator are an ion source, electrostatic accelerating system, magnetic field, vacuum system and a series of collector pockets. Most production isotope separators employ a side – extraction plasma discharge with a slit aperture ion source that produces a line image at the collector [Tak07][The79][Tra93]. The plasma is maintained by electrons emitted from a hot cathode. The ionised particles are extracted from the ion source and accelerated to their final energy in a geometry that produces a line image near the extraction slit. After being deflected by the analysing

magnetic field, the individual isotopic species are refocused at the collector defining slits. The ion beams are intercepted by collector pockets. Stable isotopes and radioisotopes can be enriched by this method. This process is not suitable for industrial separation quantities but it can allow high purities of separated isotopes.

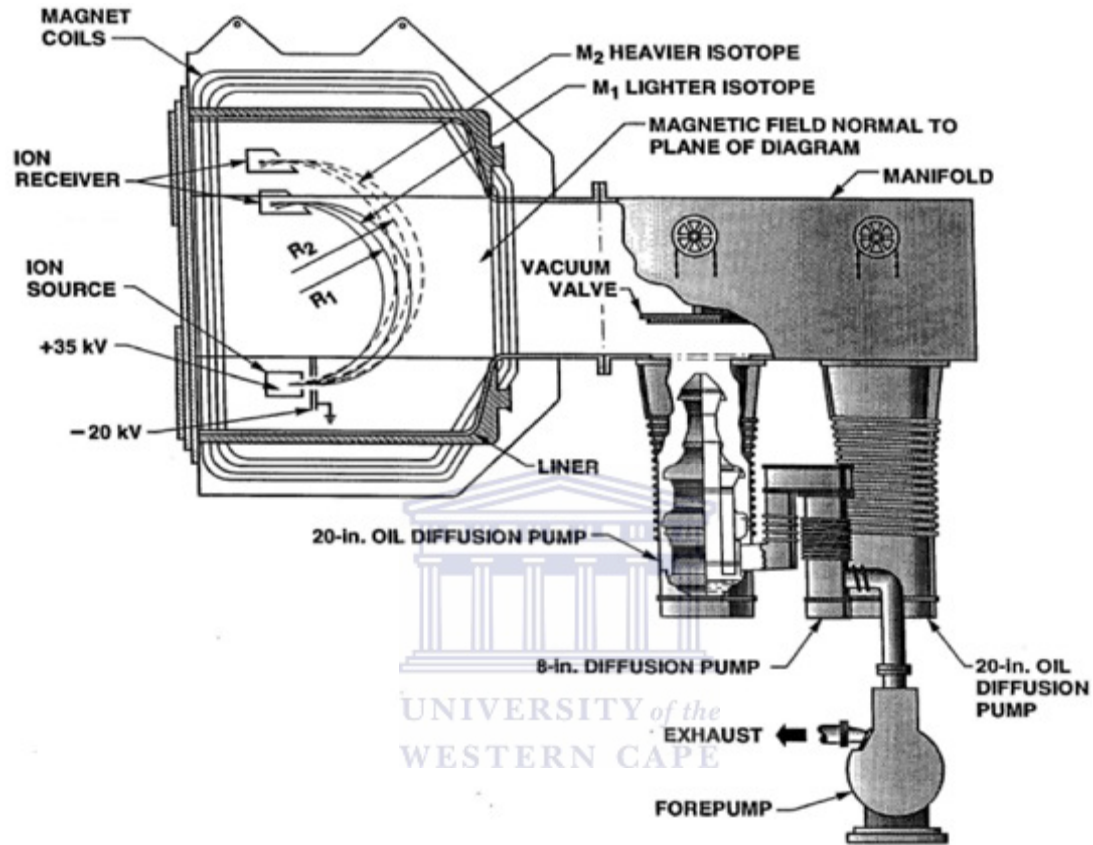


Figure 2.3: The schematic drawing showing various components of the calutron mass spectrometer for electromagnetic isotope separation process [Smi11].

2.1.4 Laser isotope separation method

The mass difference between isotopes of the same element generates slight variations in the properties of their electronic clouds. This physical fact makes it possible to separate one isotope from another by bringing an appropriate amount of coherent light energy to the atoms or molecules. This photo-excitation process, also known as laser material interaction is the first step in isotope separation process, followed by extraction and collection of the isotopically isolated material [Rou10]. In the laser

method, a laser is tuned to a wavelength which excites only one isotope of the material and ionises those atoms preferentially. The resonant absorption of light by an isotope depends on its mass and certain hyperfine interactions between electrons and the nucleus, allowing finely tuned lasers to interact with only one isotope.

Laser separation is divided into three methods: atomic vapour laser isotope separation (AVLIS), molecular laser isotope separation (MLIS) and separation of isotopes by laser excitation (SILEX) process [For83b]. In the AVLIS process atoms of a single element are ionised. See also figure 2.4 for AVLIS process schematic drawings. The basic function of the light is to remove one peripheral electron of the electronic cloud. The chemical form of the element does not change during the process. Molecular laser isotope separation (MLIS) process is carried out with molecules of a single element and the physics is based on the excitation of such molecules with enough energy to break the molecule. The basic function of the light is therefore to increase the vibrational energy of the rupture point. Energy required for such physical transformation is about 4-5 eV (electron volts). The chemical form of the photo-dissociated product changes during the process. In the SILEX process, the physics is based on extra molecular forces although molecules of the single element are involved as in MLIS. The excitation mechanisms are identical to those of MLIS, but the level of energy is lower than MLIS. This makes it cost effective when it comes to energy consumption [Rou10].

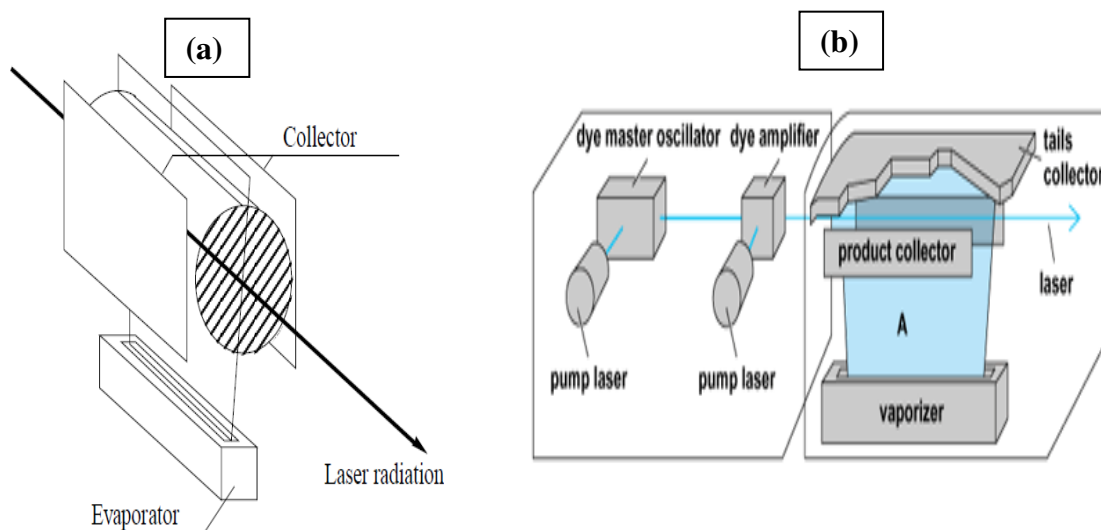


Figure 2.4: (a) A schematic drawings showing a general isotope separation by laser and (b) Atomic Vapour Laser Isotope Separation (AVLIS) process [Mai93][Fei93].

2.2 Targets and nuclear physics experiments

Nuclear physics experiments are mostly performed using energies between 5 and 25 MeV/nucleon and more for various studies. It is necessary for targets, in particular when they are made of rare isotopes, to be used more than once in different experiments if they are not damaged during use. The reasons being the high cost of isotopic material and the time required for their fabrication. During bombardment, heavy ion damage may occur on targets in two steps. When heavy ions collide with a target they can cause a transfer of kinetic energy to the targets atoms. If the kinetic energy is large, some targets atoms will be dislodged from the lattice and vacancy interstitial pairs will be formed. The target atom that is displaced after receiving the impact energy upon collision with heavy ions is called a Primary - knock on Atom (PKA). In some cases PKA's will collide with other atoms and distribute their energy throughout the target lattice until their residual energy is too low to cause further lattice displacements [Dio91].

Sometimes targets are heated up during heavy ion bombardment and as a result evaporation, melting and sputtering may become a problem [Mun89]. An example of such incidents is shown in figure 2.5(b) where bismuth target was damaged by an

intense heavy ion beam during the experiment. The SEM image in figure 2.5(a) is for undamaged Bi target by heavy ion beam. For multilayer targets on metal supports, stress can occur due to different expansion coefficients between the two materials. Therefore target characterisation before and after irradiation with a beam of particles in an experiment is of paramount importance. In addition, crucial to any study of a material is to know which elements are present and how they are distributed. This knowledge is particularly important for thin layers on the surface of a solid where trace element distributions determine such macroscopic properties as mechanical, chemical reactivity and physical [Kob82].

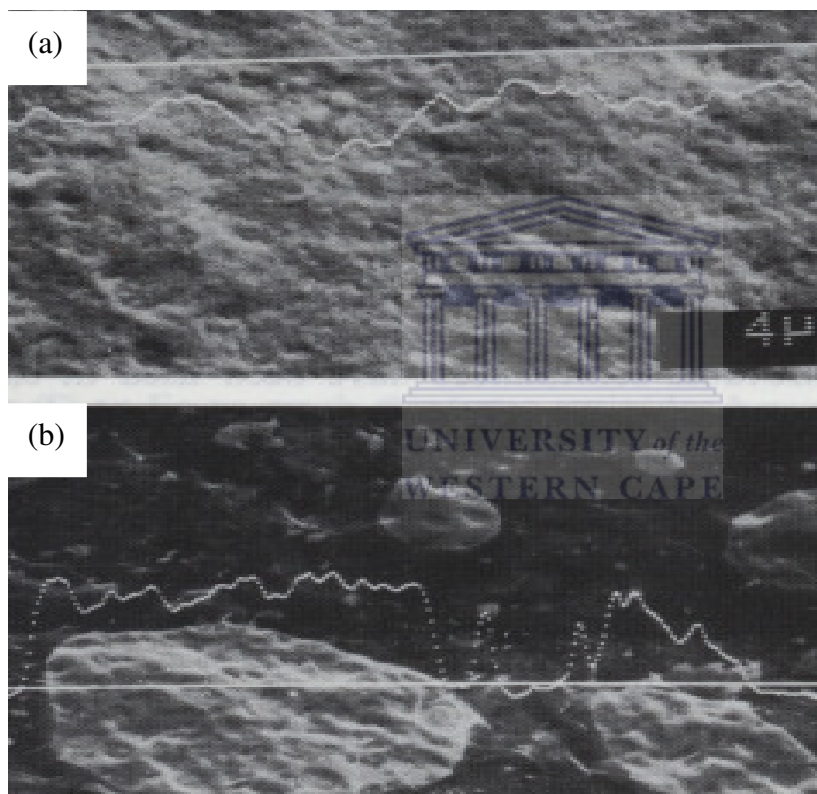


Figure 2.5: SEM images of Bi targets showing the morphology (a) before and (b) after being destroyed by the heavy ion beam. The surface topographic graphs are from the bright scan lines [Mun88].

2.2.1 Characteristics of cadmium and other isotopically enriched targets

Isotopically enriched targets have been used over the years in nuclear physics experiments at iThemba LABS. Just a few can be mentioned, especially the ones, whose manufacturing processes are challenging, e.g. zirconium. Different isotopes of zirconium have been used in various experiments at iThemba LABS. Zirconium is one of those metals which are never found as a native metal but is obtained as an oxide. Some of the isotopes are supplied in a pure metallic form and some are available as oxides. Therefore, reduction of the metal oxide to a metal before target manufacturing is necessary. The reduction process of Zr is exceptionally expensive and poses a high risk of losing the isotopic material during the process since it involves many steps [Mai89a][Abd07]. The processes like Kroll, the Van Arkel – De Boer and calciothermic reduction are some of the known reduction processes. In this particular case the focus was on ^{96}Zr which has the abundance of 2.8 %, which is less abundant when compared with other isotopes of zirconium. It should also be pointed out that Zr has a low vapour pressure and high melting point thus making it difficult to evaporate. The metal is soft and ductile though, which makes it fairly easy to work with during the rolling process. Maier reported the preparation of ductile Zr from ZrO_2 [Mai89a]. The bomb reduction technique was used to obtain metallic zirconium from a fluorine compound in which the resulting metal was further rolled down to a desired thickness.

Preparation of cadmium targets have been reported by different authors [Chi71][Bir08]. Cadmium is exceptionally volatile and does not condense on non-metallic surfaces during vacuum deposition [Mai89b][Fan08]. Biro *et al* reported the preparation of different isotopes of cadmium targets by mechanical rolling of metal ingots into thin films [Bir08]. The rolling method will be further described in the next chapter. The prepared Cd targets were self supporting and were used in gamma-ray spectroscopy experiment. On the other hand, Maier reports on preparing zinc and cadmium targets using a vacuum evaporation method [Mai89b]. The method highlighted the importance of choosing the suitable substrate and the conditions of the substrate in order to obtain a better collection. The starting materials were powders

which were mixed with tantalum powder in order to obtain a rate-controlled film condensation.

2.2.2 Nuclear physics experiments and their respective target requirements

Experiments for high energy physics are divided into three categories, depending on energy resolution needed for the experiments [Hel00]. For some experiments energy resolution is less important. Such experiments involve studies of the rare nuclei off the stability line. The study requires the reaction product to recoil out of the target nucleus to the catcher foils. In this particular case, the target thickness should be thin enough to get the maximum number of recoils out and thick enough to have an adequate production rate. Thickness also should be less than the range of the recoiling nuclei. In other experiments, the energy resolution should be between 0.5 to 1%. This energy resolution is suitable for heavy ion experiments conducted for measurements of fusion cross sections that do not involve detailed structure in the excitation functions. Studies for deep inelastic scattering, elastic scattering as well as most gamma-rays also fall under this category. Thin targets of thicknesses ranging between 50 and 300 $\mu\text{g}\cdot\text{cm}^{-2}$ are required for this type of experiments. Another requirement is that targets should have less or be free from impurities. For example, in fusion experiments the reaction products from light impurities are easily confused with evaporation residues from fusion reaction. In typical gamma-ray experiments such as Coulomb excitation or measurements, impurities are again undesirable. The reason is that the general background under peaks of interest should be low even if coincidence techniques are used to eliminate peaks arising from impurities.

There are challenges encountered in heavy ion experiments when using high resolution of approximately 0.1% keV or better. Thin and uniform self supporting targets in a range between 10 $\mu\text{g}\cdot\text{cm}^{-2}$ to 50 $\mu\text{g}\cdot\text{cm}^{-2}$ are feasible in this type of experiments and the breakage of targets is possible. It was pointed out that surface irregularity of the target of only 20 atoms represents a thickness variation of about 10 $\mu\text{g}\cdot\text{cm}^{-2}$ for a 50 $\mu\text{g}\cdot\text{cm}^{-2}$ target [For83b]. Another problem is, as the mass of the incident projectile increases straggling and multiple scattering are encountered. This

limits the energy resolution even in the thinnest self supporting target. Therefore, various isotopically enriched targets that have so far been prepared for use in different nuclear physics experiments described. Ueta *et al* [Uet97] used ^{88}Sr , ^{90}Zr and ^{92}Mo to study of the isotopic and isotonic dependence of the nuclear ion–ion potential.

Targets made from enriched isotopes of $^{10,11}\text{B}$ were used for fusion reaction measurements by Ueta *et al* [Uet97] and in various nuclear institutes for neutron physics measurements [Jan83]. Sletten and Knudsen [Sle72] reported the preparation of targets of $^{90-96}\text{Zr}$ and ^{182}W for use in high–resolution spectroscopy at the Niels Bohr Institute in Copenhagen, Denmark. The aim was to use the minimal quantity of the initial isotopic materials [Sle72]. Experiments where charged particles or electrons focused on or transported to a detector are examples of accelerator- based studies, which can be made with targets that contain small amounts of isotopic target material. For this kind of studies it has then become possible to extend the domain of potential target materials to species which are very rare or unstable and undergo radioactive decay. Targets of $^{152,154}\text{Eu}$, ^{249}Bk , ^{151}Sm and ^{148}Gd were used in such application for nuclear spectroscopy studies [Lan87]. Adair reports on fabrication of radioactive isotopes of tritium targets used by researchers as a source of neutrons [Ada78]. Subsequently, these neutrons were later used in material irradiation and in testing experiments. Gas targets like ^3He were also used in different experiments with beams of fast charged particles [Wal62].

2.3 Techniques for targets manufacturing

Targets are prepared using various methods depending on the chemical and physical properties of materials to be used. Methods are also chosen by considering the requirements of the targets for the particular experiment in terms of thickness, size and how much impurities can be tolerated.

2.3.1 Multiple painting method

This procedure is preferred whenever the requirement for homogeneity and chemical impurities of a target are not extremely important. The method involves brushing an organic solution of an actinide nitrate or any metal nitrate on a backing plate which is normally aluminium with a thickness that will withstand the required number of annealing operations. This is followed by drying and tempering of a backing plate in a muffle furnace. The organic compounds are burned off during this process leaving the layer of the metallic foil on the surface of the backing plate. This procedure is repeated until the required thickness is achieved. Although the method is simple for producing strong targets that are not fragile under influence of a beam, they are chemically impure and not uniform in thickness. Therefore it limits their application when high resolution accelerators are used [Sin83].



2.3.2 Depositions methods

Depositions methods which are mostly used in target making are physical and chemical vapour deposition. Chemical vapour deposition (CVD) or vapour plating is a precipitation of thin films from the gaseous phase and thus shows some analogy to the evaporation condensation procedure. The commonly applied methods are those involving pyrolytical decomposition of the gas onto a hot surface or dissociation of a gas in a glow discharge resulting in a thin film deposition on the electrode. The CVD was used in the beginning of targetry to prepare isotopically enriched targets of boron from B_2H_6 gas as well as enriched $^{12,13}C$ from C_6H_6 gas. The same method was also used to prepare tungsten targets [Glo65]. The method though yields brittle targets with a minimum thickness [Gal83].

Kuehn *et al* used electroplating also known as molecular plating method for manufacturing of self supporting chromium targets which are difficult to produce with other methods [Kue72][Hin72][Ver72]. It is also reported by Cecchi and various authors for the manufacturing of ruthenium targets and in thin film technology [Sed72] [Cec88] [Glo72]. The method has also been reported by Eberhardt *et al* for

the preparation of lanthanide and actinide targets using organic solvents in vertical deposition plating set up cell [Ebe04]. Although the method produced satisfactory results, the homogeneity in thickness was of concern. To improve the homogeneity of the deposited foils, Liebe *et al* reported on continuation with Eberhardt's work by using the same procedure, however with a horizontal deposition plating cell [Lie08]. The typical plating cells set up mentioned are shown in figure 2.6. Heagney reported that the method can also be used for the reduction of certain isotopic compounds to obtain the starting material for other fabrication methods [Hea72]. The disadvantage of the method is that it produces foils of poor uniformity and purity.

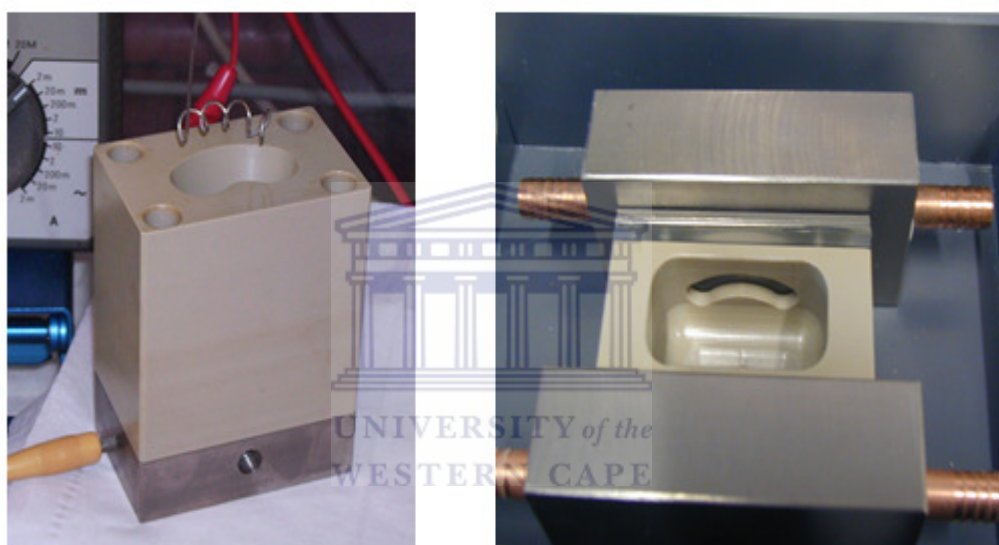


Figure 2.6: These are two pictures of typical electroplating cells. The plating cell on the left is for vertical plating and on the right is the modified design which uses horizontal plating type [Ebe04][Lie08].

2.3.3 Vacuum evaporation technique

The principle of the vacuum evaporation condensation involves heating material to be deposited using an evaporation source up to a temperature which causes the generation of a vapour cloud. This vapour cloud propagates in vacuum towards the substrate, where it is condensed in the form of a thin film. In targetry, the thin film needs to be deposited in a manner permitting separation from a substrate.

Both metals and thermally stable compounds are vaporized readily under vacuum conditions by heating them to a temperature which raises their vapour pressure to a level greater than 10^{-2} Torr. There are two different types of vaporisation sources used for target preparation [Ang84]. The hot crucible source provides an indirect heating of the material from a shaped refractory metal receptacle which is heated by resistive techniques. With the cold crucible approach, the copper crucible is water cooled and the evaporant is directly heated by electron bombardment in the process. Evaporation by using these two types of sources can be used for most of the target material covering range of temperatures. The disadvantage is that it uses excessive amounts of materials, which become costly when isotopically enriched targets are manufactured.

Another method used for thin film deposition is focused ion beam sputtering (FIB) [Bau79] [Mai91b]. In targetry only the focus ion beam sputtering mode is of interest which was introduced to the field by Sletten and further investigated by Scaif, Wirth, Kwinta and Folger [Sle72][Sca75][Kwi79]. In sputtering the formation of the atomic particle beam propagating toward the substrate is accomplished by a collision cascade mechanism which does not require or imply an elevated source temperature. The abrasion rate is a material constant and is nearly independent of temperature. Typical sputtering yields are of the order of magnitude of 0.5 to 5 atoms per incident ion for practically all elements and compounds under realistic operating conditions. Thus sputtering offers a convenient method to prepare thin films of refractory materials such as Ru, Ta, W, Re, Os, Ir and Pt as well as of the actinide elements and their oxides. High collection efficiencies of 70% were reported in favourable conditions. There are two major factors that govern the total efficiency of sputtering in target preparation. One factor is the sputtering yield defined as the number of atoms driven out of the sample per bombarding inert gas. The other factor is complex and involves the solid angle, the angular distribution of emitted atoms and the condensation probability for the atoms on the desired substrate surface [Mai91a]. Since it is done at room temperature, the sputtering method offers an advantage in manufacturing targets with high melting points like tungsten without damaging the parting agent. The condensation efficiency is low according to Maier-Komor, about 0.3% with a minimum crucible to source distance of 7 cm [Mai91b].

Pulsed laser beam method is also used in targetry as a deposition method and first reported by Maier-Komor [Mai91c]. The method involves focusing the beam through an entrance window into a vacuum chamber on very small samples with a mass of less than 1 mg. Maier-Komor found the method to have a high yield when compared to the electron gun system and heavy ion sputtering. The method is mostly preferred when relatively expensive isotopes are used. The disadvantage of the method is the light reflectivity of many metals, which reduces the power input remarkably. Another method that was recently discovered in targetry involve the use of a mebrane filter of anopore aluminum oxide disc (Anodisc) as a support and filtering mebrane. The method involves dissolving the target material in a solvent which is later filtered using the Anodisc. It was applied on manufacturing of ^{238}U target. This method was reported to have 100% chemical yield [Tak07].

2.4 Techniques used in target characterisation

Manufactured targets need to be further investigated in order to determine their thickness and elemental analyses. The important piece of information in targetry is the thickness since all the relevent calculations pertaining to the beam energy and current to be used during the experiment are based on it. However, in lifetime experiments, e.g. using Doppler methods as mentioned ealier, the target must have a specific thickness [Lie09][For83][Mai81]. The success of such experiments depends on the correct target thickness. Methods like alpha spectrometry, microprobe methods and X-ray fluorescent methods are common techniques used to measure the thickness [Mun89] [Kat69][Lor89]. Other aspects that need to be known in manufactured targets are their topography, morphology, crystallographic information as well as impurity content and distribution. It is advisable that target characterisation be done before and after the experiment as it is mentioned ealier, especially when targets need to be used more than once.

The typical methods like XRD, SEM and AFM were used to determine the crystal structure, topography and morphology of the thin films in this study. The full description of the methods will be given in detail in the next chapter. Minimisation of

impurities in the targets is crucial as unwanted peaks will be minimal in the experimental data. Dollinger *et al* reported on investigating the concentration profiles of light elements in thin films and foils at surfaces and interfaces. The contamination of carbon films produced using vacuum evaporation method by hydrogen and its compounds were investigated by using depth- of- field microscopy to scan the hydrogen profile [Dol93]. It was concluded that the contamination was caused by adsorption of hydrogen or water at the surfaces of carbon foils.

Methods like Ion induced Auger electron spectroscopy(IIAES) are also used to get an information of surface contamination of thin films [Lor89]. A depth scale deduced from Auger lines can distinguish between the physically adsorbed and chemically bound elements. This method is quantitatively useful to analyse and monitor the sample during an experiment. Bulk sensitive methods like Rutherford backscattering (RBS) and Rutherford forward scattering (RFS), elastic recoil detector analysis (ERD) were reported for target characterisation[Kat69][Lor89]. Target impurities were also investigated by Pal *et al* by using X-ray emission [Pal93].

Other target materials cannot be deposited directly to a substrate because of various reasons regarding their crystal structures. For instance, sometimes silicon need to be deposited onto a metal support to prevent stress on silicon during deposition. Alternatively, it can be deposited directly onto another film that serves as a support and if it is needed as a self supporting target, then the support needs to be etched off using chemicals. The appropriate metal for this is copper. Meens *et al* [Mee93] were interested in determining the copper contamination on thin silicon films prepared by various vacuum evaporation methods. Vacuum evaporation with different evaporation parameters and using ion beam sputtering for heating were utilised for this comparative study. Liebe *et al* performed the characterisation of the manufactured radioactive targets as a comparative study using electroplating cells with different target positions [Lie08]. The analysis of the deposited films were conducted using neutron activation analysis (NAA) for thickness determination.

Surface morphological investigation and chemical composition were conducted by scanning electron microscopy (SEM) and energy dispersive X-ray (EDX), respectively. The microstructure of deposited multicoatings of metal films were

investigated by transmission electron microscopy (TEM) and the selected area electron diffraction (SAED) method [Mee93]. RBS and NAA analysis were specifically used for thickness determination and copper contamination on silicon foils. Results showed that copper contamination increased with temperature increase. See figure 2.7 for RBS spectrum below. Methods like energy dispersive X-ray, optical and electron microscopy are also used on film technology in order to obtain information on target thickness, crystal structure and homogeneity [Mai81][Lie08].

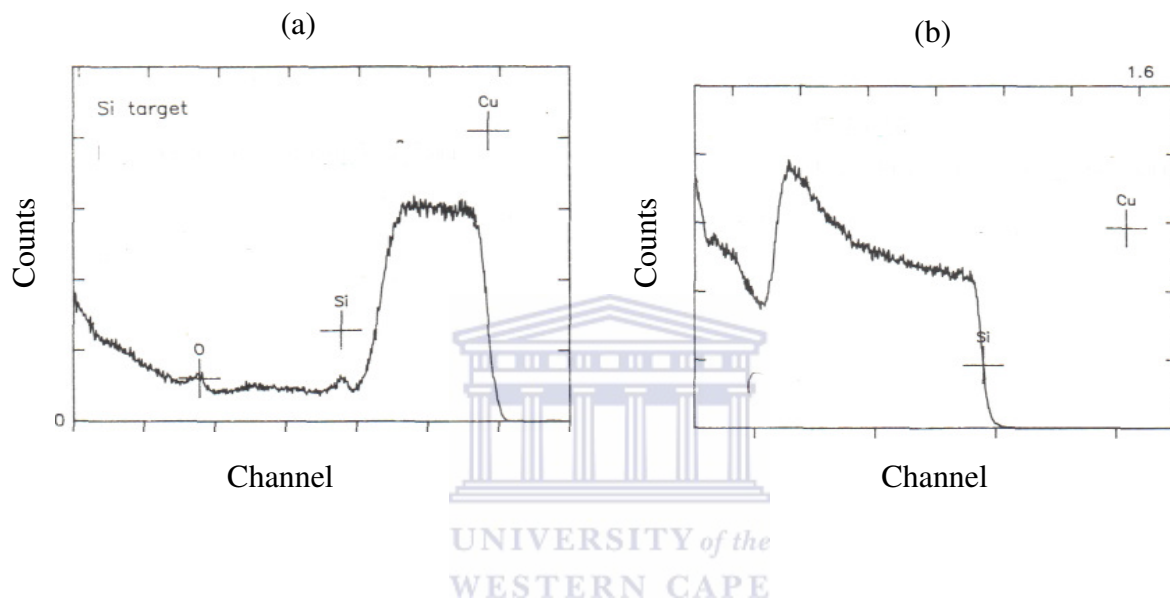


Figure 2.7: The RBS spectra of Silicon target (a) contaminated with copper and (b) free from copper contamination [Mee93].

CHAPTER 3 MATERIALS AND METHODS

The main aim of this study was to manufacture targets of isotopically enriched ^{114}Cd with different thicknesses. Targets were manufactured by vacuum evaporation using resistive heating method to heat a tantalum boat source and mechanical rolling. Thereafter the rolled films were mounted on frames (see also figure 3.3) for use in AFRODITE experiments (figure 3.4). The type of nuclear physics experiments performed in the AFRODITE facility also depends on target thickness; hence the thickness was accurately determined prior to the target being used. Further analyses using analytical techniques were conducted and are discussed in detail in this chapter. Most of the characterisations were conducted on the semi-thick target since this was the main required target of the experiment. This is explained in subsection 3.1.2 under applications of cadmium target. This chapter is divided into two sections where techniques used during target manufacturing are discussed in section 3.1 while the characterisation methods are discussed in section 3.2.

3.1 Manufacturing of targets

Cadmium is volatile and has a high vapour pressure and makes it uncontrollable once heated. Secondly, targets were needed as pure and self supporting for an experiment. Other methods like electrodeposition and painting were not suitable because of impurities that will be introduced by deposition solvents. The target laboratory has two vacuum evaporators using electron and resistive heating vacuum evaporation sources. These methods are chosen to melt the materials depending mostly on materials physical properties such as melting point and the vapour pressure. Since cadmium has a low melting point and a high vapour pressure, controlled working conditions under vacuum were needed. Therefore, vacuum deposition method using resistive heated source was considered for cadmium deposition. To proceed with the preparation of ^{114}Cd targets, the method was firstly developed using a natural material of zinc for vacuum deposition purpose.

Zinc was chosen because it has physical and chemical properties similar to that of cadmium and it was available in a metal powder as the cadmium isotope. Both the zinc and the supplied isotopic material of cadmium were in the form of a powder. The parameters inside a vacuum chamber were alternated until a better layer of the deposited zinc metal was achieved. The crucial parameters during the deposition were working pressure, voltage and source-to-substrate distance. The whole process was fully dependent on the working pressure, since the materials can be melted at lower temperatures in high vacuum in the range of 10^{-5} mbar. If lower temperatures are used, then source-to-substrate distance can be shortened. And this can increase the collection yield of the material. In addition, different types of substrates were also used during the development of the method. Substrates like glass, and metals such as molybdenum, tantalum and copper were used. This was repeated until a better yield of about 90 % of the deposited zinc metal was achieved. Then the method was fully adapted and applied during the manufacturing of the enriched cadmium targets. This process was done as the method cannot be developed using isotopic material since it is supplied in small quantities at high cost.

Prior to vacuum evaporation, the isotopically enriched metal powder of ^{114}Cd (90.01% of an isotope) was compressed into a pill using a compact hand operated pellet press. Powder compressing improves the physical contact of the powdered materials and excludes much of the adsorbed gases which may cause spitting of the material when heated up during deposition process. A polished copper block was used as a substrate and it was continuously cooled by water to prevent overheating of the block and the deposited ^{114}Cd metal as it was held closer to the heated tantalum boat. The temperature of the substrate was believed to be 5 or 10 °C above ambient since no direct temperature measurements were conducted. Copper was chosen as a substrate because cadmium deposits easily onto metal surfaces and the metal has a good cooling effect.

Vacuum deposition of cadmium was conducted by heating the tantalum boat, as a source, containing the material by resistive method, see fig. 3.1. To control cadmium vapour since the metal is volatile and for better collection of evaporated metal, the Ta boat was designed so that the vapour escapes in about 2 mm diameter opening of the

boat. The process was carried out until it reached a condensation stage where atoms of ^{114}Cd were collected to a copper block. The deposition process was monitored by the quartz crystal thickness monitor as the process had to be discontinued when no reading was showing on the monitor. The whole purpose was to deposit all isotopic material placed into the boat for a better yield. The high vacuum of the system was supplied by two dedicated pumps; diffusion and the mechanical pumps. The mechanical pump reduces the pressure inside the chamber to 10^{-3} mbar while the diffusion pump further reduces the system to the high vacuum of 10^{-5} mbar.

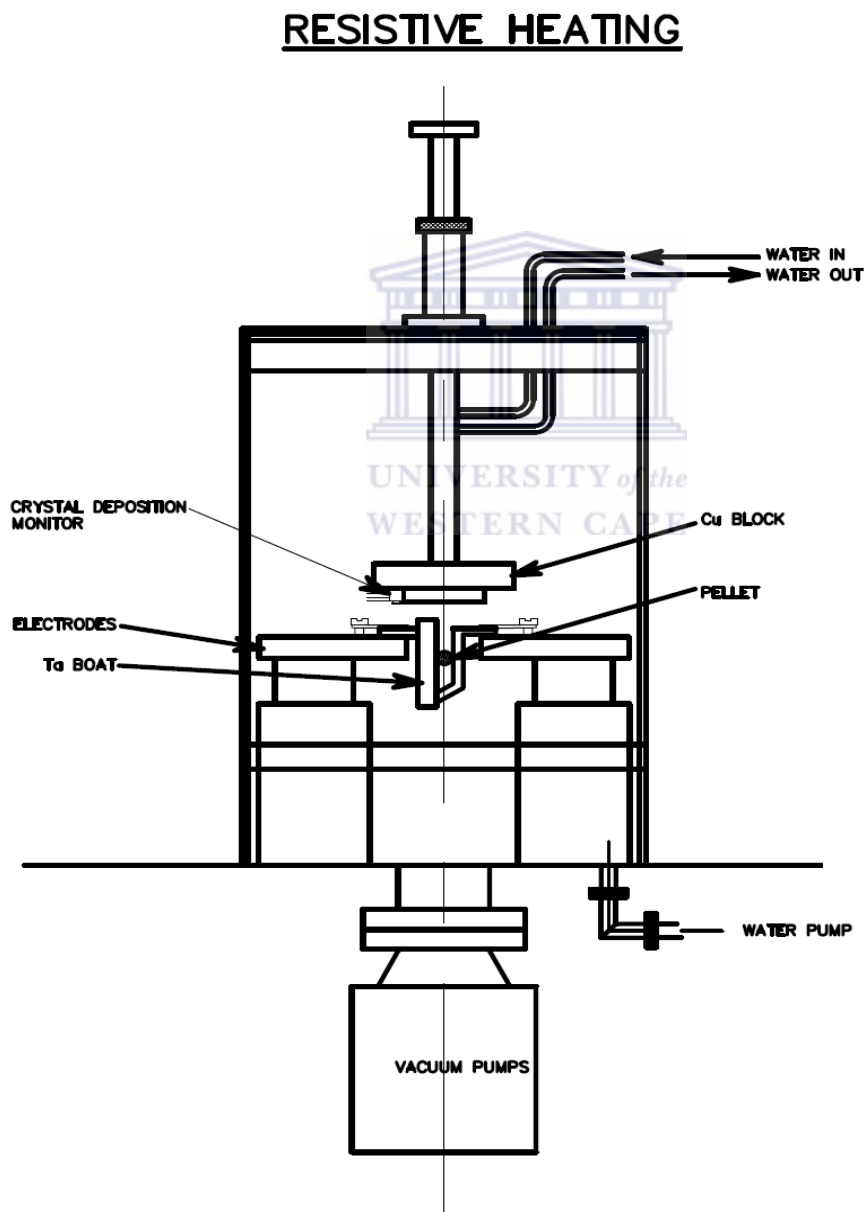


Figure 3.1: Schematic drawing of a resistive heating vacuum evaporator used to deposit ^{114}Cd .

3.1.1 Rolling of metallic ^{114}Cd

The rolling method is mostly applied in targetry when thicker targets are required, or when the target material is too small to be used in other processes like vacuum evaporation (see an example in figure 3.2) [Kar72][Kaz05]. It is also preferred when isotopic materials are used as they are supplied in small quantities. Cadmium metal collected after the deposition process was further rolled down to thinner films using an all speed rolling mill. Polished stainless steel plates were used as the carrier of cadmium in between the rolling mills, see also figure 3.2. The preferred shape was the envelope as it allowed easy handling and no materials are lost to the mills (figure 3.3). This is referred to as rolling pack. Cadmium metal was rolled under ambient temperature as the material is ductile and no heat is required for treatment. The metal is so soft that the cadmium metal sticks onto rolling plates. To prevent the cadmium sticking during rolling, double pack plate rolling was used. This was achieved by inserting an old stainless single pack (being used before) to a new pack. Used plates tend to be smoother on the polished side than the new ones. The same method was also reported by Fan [Fan08] during their rolling of cadmium and zinc metals.

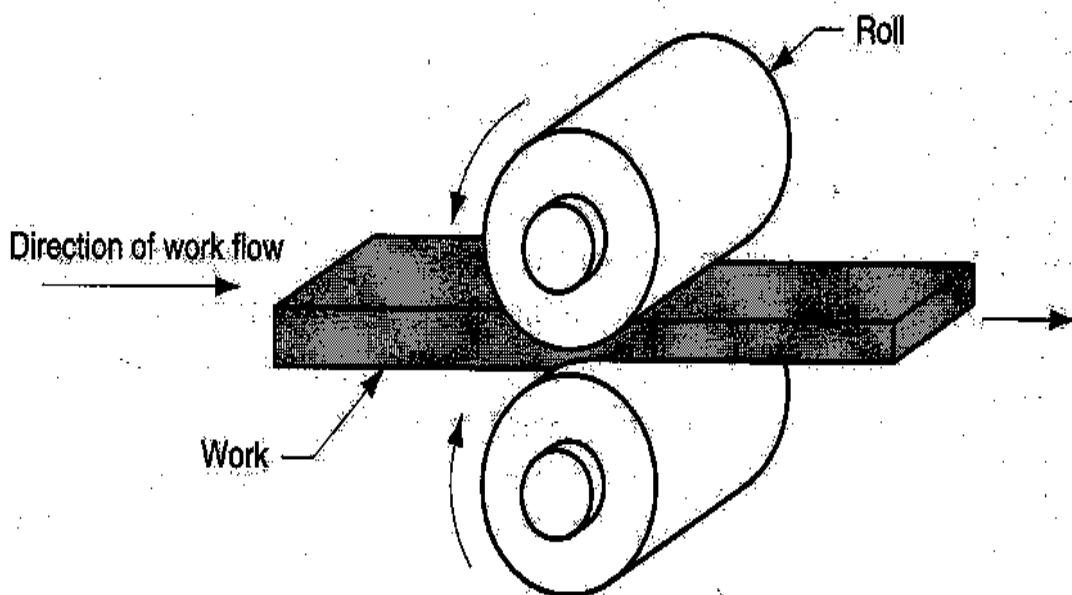


Figure 3.2: A schematic diagram illustrating a rolling process [Gro99].



Figure 3.3: Polished stainless steel plates of an envelope type showing, from right to left, the shape deformation after several strikethrough in mills.

3.1.2 Application of ^{114}Cd targets

Self-supporting targets were mounted on frames and placed on a target ladder to be used in the AFRODITE gamma detector array at a separated sector cyclotron (SSC) using a Doppler-shift attenuation method, as shown in figure 3.4. It was required that the target thickness and homogeneity for a given experiment be measured accurately before the experiment. The target thickness required was such that the nuclei of interest should slow down inside the target before being released into vacuum. For the determination of this optimal target thickness, referred to as semi-thick, Monte Carlo calculations were carried out using COMPA and GAMMA codes. In the COMPA program, it simulates the slowing down of the projectile in a target, the reaction kinematics for the produced compound nuclei, the particle emission and the entry-state population distribution for the final nucleus. Furthermore, the cross-sections for the various reaction channels are calculated. For each recoil geometrical positions at

which it is produced in the target, the initial velocity and direction as well as the excitation energy and the transferred angular momentum are calculated.

Whereas the GAMMA program simulates the slowing-down process and nuclear scattering of the recoils in the target, the emission of γ -ray cascades from the entry state to the level of interest and the registration of the γ -quanta in the detector system. When the recoils escape from the target into vacuum, it is treated the same way as a second target layer. Multiple scattering of the recoils is described in the program GAMMA by a model function which is suitable for small angle scattering only. The large angle scattering is calculated by dividing the recoil trajectory into 10 – 100 segments with lengths of approximately 100 – 200 $\mu\text{g}\cdot\text{cm}^{-2}$ for high recoil velocities which reduce to 20 $\mu\text{g}\cdot\text{cm}^{-2}$ for low velocities. This procedure gives an adequate description of the γ -lineshapes even when the Doppler effect is caused mainly by multiple scattering [Lie09].

To determine the optimal target thickness, the Doppler – shift attenuation factor was calculated for the lifetimes for the nucleus of ^{136}Nd . The calculations were carried out for target thicknesses of 0.5 – 10 $\text{mg}\cdot\text{cm}^{-2}$. The sensitivity of the electronic stopping power was determined and the largest determination of the stopping-power parameters lies between approximately 2.5 and 5 $\text{mg}\cdot\text{cm}^{-2}$ with the maximum at a 3.65 $\text{mg}\cdot\text{cm}^{-2}$. This thickness (3.65 $\text{mg}\cdot\text{cm}^{-2}$) was chosen for the ^{114}Cd target to be used in a stopping power measurement [Lie09]. The thick target, 12.8 $\text{mg}\cdot\text{cm}^{-2}$ was used during the stopping power experiment for the analysis of the Doppler lineshapes. The recoils were fully stopped in this target so that transitions deexciting levels of large lifetime show instrumental lineshapes of the unshifted γ -lines. The analysis of this data set demonstrated that the chosen transitions indeed show instrumental lineshapes, providing evidence that the lifetimes of the initial states were large enough to apply the semi-thick target method.

The targets were bombarded with a beam of silicon-28 (^{28}Si) ions with energy of 155 MeV during the stopping power experiment. The purpose of the experiment was to obtain experimental information on the stopping-power parameters of ^{138}Sm , ^{137}Pm and ^{136}Nd nuclei in a ^{114}Cd target using a semi-thick target method [Lie09]. Findings

of the experiment are discussed in detail in the published paper, [Lie09]. Another important aspect was that the thickness remains unchanged during the irradiation process and after exposure to the high beam current. Moreover, targets were further characterised for thickness and topography and the methods used are discussed in details in the follow-up section 3.2. Figure 3.5 show the images of targets after the experiment.

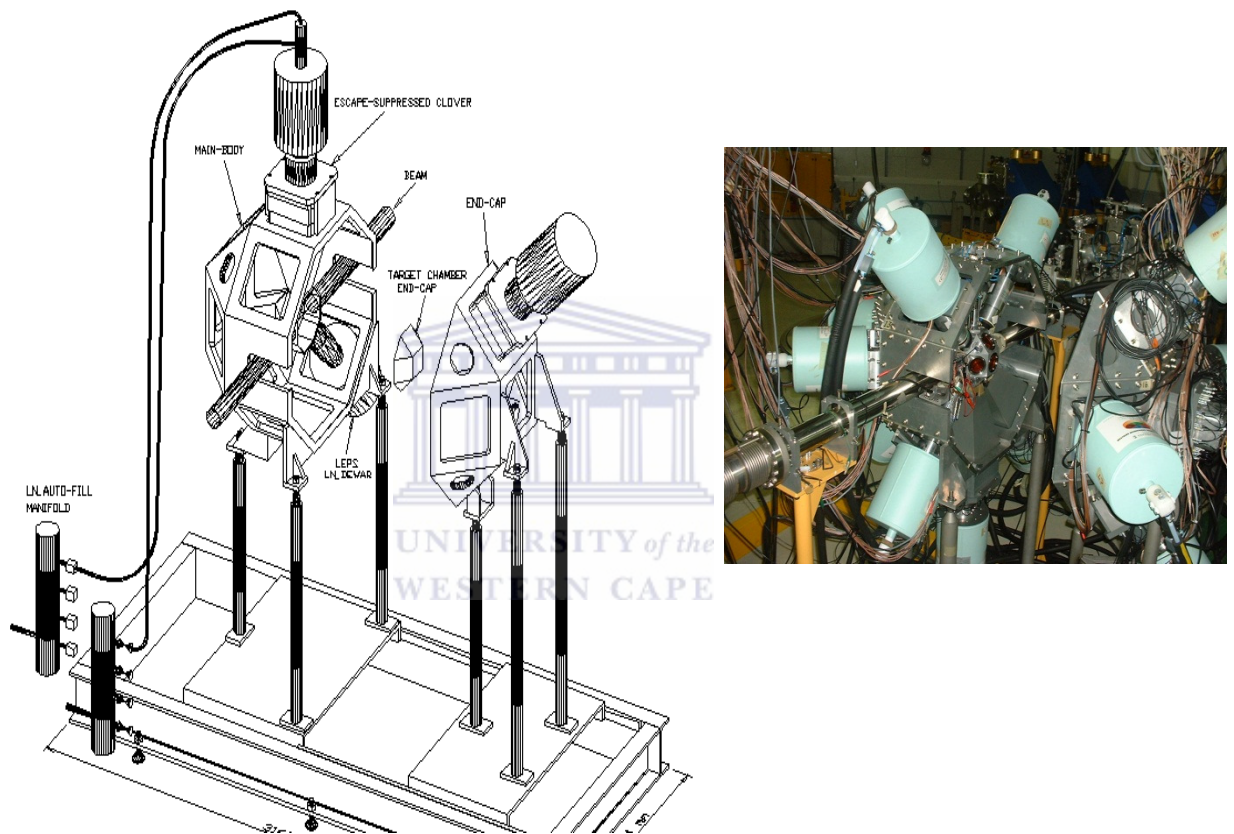


Figure 3.4: Schematic diagram of the AFRODITE instrument (left) and the image (right) showing the target chamber, clover detectors and the beam line.

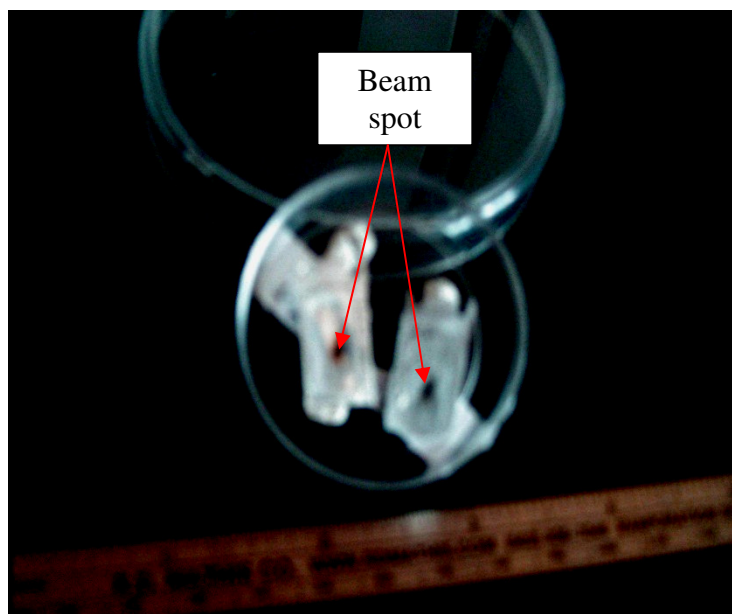


Figure 3.5: Two Cadmium targets with beam spots produced after irradiation with ^{28}Si beam. Targets were produced by vacuum deposition and rolling.

3.2 Characterisation of ^{114}Cd targets

Other aspects as present constituents in a target, thickness homogeneity and to observe if the cadmium material was not sputtered off during the experiment were also investigated. These were determined using RBS and PIXE for elemental analysis, AFM and SEM for surface topology and morphology and XRD for crystal structure.

3.2.1 Rutherford backscattering (RBS)

The thickness measurements of the cadmium targets were performed at iThemba LABS in the nuclear microprobe (NMP) facility located at the Material Research Department (MRD). A microprobe is installed on a 6MV single - ended Van de Graff accelerator. The Rutherford backscattering (RBS) method was used only for the measurement of the semi-thick target. The RBS technique is based on the backscattering of energetic ions incident on a sample surface [Sch98]. It involves

measuring the number and energy of ions in a beam which backscatter after colliding with atoms in the surface and near-surface regions of a sample at which the beam has been directed. The kinematics of the atomic collisions occurring at a sample surface is simplified by treating the target atom as a freestanding atom, and so the interaction is described as a simple two-body collision [Woo84]. Fig. 3.6 is a schematic illustration of a collision between an incident ion of mass M_1 and energy E_0 and an atom of mass M_2 initially at rest on the sample surface.

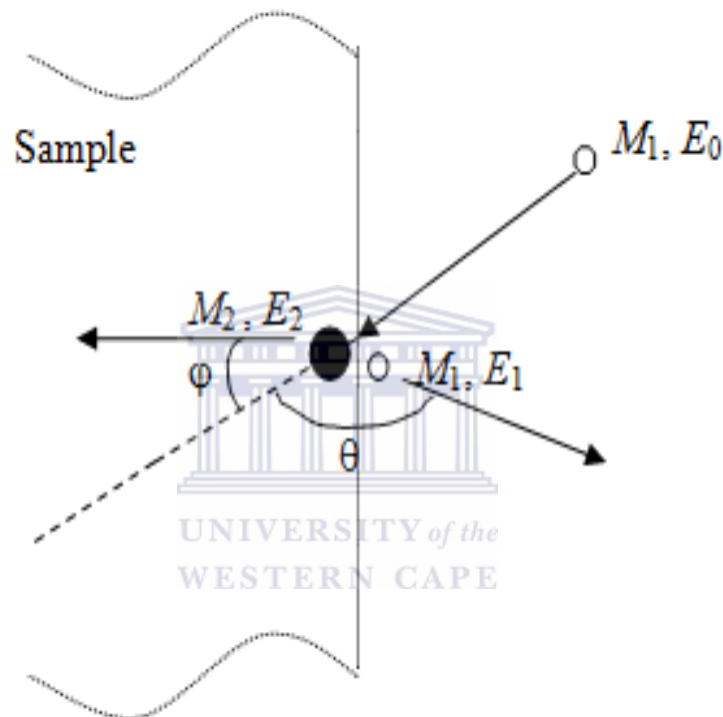


Figure 3.6: A schematic representation of a Rutherford backscattering process at a sample surface [Woo84].

The incident particle is backscattered at an angle θ to the incidence direction with a reduced energy E_1 and the target atom recoils at an angle ϕ to the incidence direction with a recoil energy E_2 . The angles θ and ϕ are measured from the incidence direction as illustrated in Fig. 3.6. The ratio of the backscatter energy to the incidence energy is defined as the kinematic factor K . Conservation of energy and momentum in the directions parallel and perpendicular to the incidence direction in Fig. 3.6 leads to the following expression for the kinematic factor [Sch98];

$$K = \frac{E_1}{E_0} = \frac{\left[\sqrt{1 - (R \sin \theta)^2} + R \cos \theta \right]^2}{(1 + R)^2} \approx 1 - \frac{2R(1 - \cos \theta)}{(1 + R)^2} \quad (3.1)$$

where $R = \frac{M_1}{M_2}$. The approximation holds for $R \ll 1$ and θ close to 180° .

During an experiment, a proton beam was accelerated vertically downwards and passed through a 90° analysing magnet to the highly evacuated beam line. To avoid the scattered proton beam entering the chamber, the beam is focused using the quadrupole lenses. The distance the proton travels is 15 m before reaching the target chamber. This 15 m distance makes it possible to obtain the ultimate beam spot sizes. Knowledge of the number and energy of the backscattered ions makes it possible to determine the atomic mass and elemental concentration of the backscattering species from the surface to a few micrometres into the sample bulk [Fle95][Msi06]. Targets were irradiated by focused beam of $^4\text{He}^+$ supplied by the 6MV single ended Van de Graff accelerator. The energy of the beam was 2 MeV with a current of 4.000 nA with a charge of $20.000\mu\text{C}$. An annular Si surface barrier detector, positioned at an angle of 176° to the incident beam was used to register the backscattered protons. The detector resolution was 30 keV for 3 MeV protons.

The measurements were carried out in a scanning mode with a defocused beam to cover a larger area and to avoid local heating of the sensitive target. The size of the beam spot was $1\text{ mm} \times 1\text{ mm}$. This analysis was performed before and after the stopping power experiment. RUMP, Rutherford computer simulation software package was utilized for the RBS spectra simulation [Doo86]. The RBS spectrum is a plot of backscattered ion intensity against ion energy. It can be noted from Eq. (3.1) that ions backscattered from the surface have energy, which for a specific angle of scatter, is defined only by the ratio of the masses of the incident ion and the scattering particle. This forms the basis of elemental identification in RBS [Sch98]. The unknown mass M_2 is calculated from the measured energy E_1 through the kinematic factor. The peak height of the ion intensity is an indication of elemental concentration [Gal04]. The elastic scattering cross-sections of atoms for the typically high energy ($\sim\text{MeV}$) ions used in RBS are relatively small [Mag82], therefore energy losses due to multiple atom scattering are small.

Coulombic interactions with electrons cause no deflection of the ions but linear deceleration [Gal04]. The rate of energy loss is thus essentially constant so that different energy losses can be related linearly to depth below the surface. This means that for a given scattering species the size of the signal as prescribed by the kinematic factor can be related to the composition at the surface [Mag82]. The size of the signal at lower energies is due to the composition at a depth below the surface proportional to the energy loss. In short, the energy width of a peak can be used to determine film thickness if the energy loss per unit length (energy loss factor) in the given sample matrix is known [Pro95].

3.2.2 Particle induced X-ray emission (PIXE)

For thickness determination of thick target, particle induced X-ray emission (PIXE) was used as the higher energy beam was required. In PIXE measurements, charged particles (protons, alpha particles or heavy ions) are used to create inner-shell vacancies in the atoms of the specimen. Filling the vacancies by electrons from the outer shells leads to the emission of characteristic X-rays (and/or Auger electrons) and this forms the basis for a highly sensitive elemental analysis. Protons of 1 - 4 MeV energy are mostly used. Their slowing down in matter is smooth and well characterized, with little scattering and deflection. The process is therefore easy to quantify. X-ray production yields are high and the continuum background in PIXE is low. Therefore the detection limits are about two orders of magnitude better than with electron beams. PIXE spectra are usually collected in energy-dispersive mode and all elements with atomic numbers above 10 (Na and above) can in principle be detected at once. The characteristic X-rays of lighter elements are absorbed in the windows of routinely used Si (Li) or high purity germanium (HPGe) detectors. Typically reported sensitivities are 10 - 20 ppm for Na to Cl and 1 - 10 ppm for Ca and heavier elements. No information related to chemical identity, coordination chemistry or oxidation state of a particular element could be directly obtained. The elementary analysis of ^{114}Cd was performed by PIXE and the data was collected using the XSYS acquisition system and processed using GeoPIXE II [Fle95]. A proton beam of 3.0 MeV and current of 50 to 100 pA was focused to a 3 μm x 3 μm spot size and raster scanned

over selected areas of interest. The number of pixels was of 128 x 128 over a surface area of $250 \times 250 \mu\text{m}^2$. X-rays were collected by a Si (Li) detector whereas the scattered particles were detected by a surface barrier detector. Elemental maps exhibiting patterns of the metal distributions were generated using dynamic analysis method developed by Ryan and Prozesky [Rya01, Pro95].

3.2.3 Surface characterization by atomic force microscope (AFM)

The AFM is a high resolution type of scanning probe microscope, with demonstrated resolution of fractions of a nanometer. The AFM is one of the foremost tools for imaging, measuring and manipulating matter at the nanoscale. The principle involves gathering the information by tracing or feeling the surface of a material using a mechanical probe. The instrument comprises a microscale cantilever with a sharp tip at its end that is used to scan the specimen surface. The cantilever is typically silicon or silicon nitride with a tip radius of curvature on the order of nanometers. When the tip is brought into proximity of a sample surface, forces between the tip and the sample lead to a deflection of the cantilever. Depending on the condition, forces that are measured in AFM include mechanical contact force, Van der Waals forces, capillary forces, chemical bonding, electrostatic forces, magnetic forces, Casimir forces, salvation forces etc. Typically, the deflection is measured using a laser spot reflected from the top of the cantilever into an array of photodiodes. Other methods that are used include optical interferometry, capacitive sensing or piezoresistive AFM cantilevers. These cantilevers are fabricated with piezoresistive elements that act as strain gauge. Using a Wheatstone bridge, strain in the AFM cantilever due to deflection can be measured, but this method is not as sensitive as laser deflection or interferometry.

The AFM can be operated in a number of modes depending on the application. In general, possible imaging modes are divided into contact (static) modes and a variety of dynamic modes (non-contact mode). In the contact mode operation, the static tip deflection is used as a feedback signal. Because the measurement of a contact signal is prone to noise and drift, low stiffness cantilevers are used to boost the deflection signal. However, close to the surface of the sample, attractive forces can be quite

strong causing the tip to snap-in to the surface. Thus contact mode AFM is almost always done in contact where the overall force is repulsive.

In contact mode, the force between the tip and the surface is kept constant during scanning by maintaining a constant deflection. The non-contact mode operation involves oscillating the cantilever externally at or close to its resonance frequency. The oscillation amplitude, phase and resonance frequency are modified by tip sample interaction forces. These changes in oscillation with respect to the external reference oscillation provide information about the sample's characteristics. Schemes for the dynamic mode operation include frequency modulation, amplitude modulation and tapping mode. Moving to a tapping mode also known as Intermittent Contact Mode, the cantilever is driven to oscillate up and down at near its resonance frequency by a small piezoelectric mounted in the AFM tip holder. The amplitude of this oscillation is greater than 10 nm, typically 100 to 200 nm and decreases due to the interaction forces acting on the cantilever when the tip comes close to the surface of the sample. Therefore the image is produced by imaging the force of the oscillating contacts of the tip with the sample [Mag82] [Gal04].

The AFM analyses on a semi-thick target were performed at the Material Science Research Department at iThemba LABS employing the Nanoman-Veeco AFM for surface characterization of cadmium targets. The instrument has the imaging capabilities in both contact and tapping imaging modes namely Electric force imaging, magnetic force imaging, height, phase and amplitude imaging. The Nanoman-Veeco AFM has an integrated optical microscope with a magnification range of 410-1845, corresponding to a field of view of 180 – 810 μm , which is most useful for alignment of targeted surface features. The integrated optical microscope is also capable of taking snapshot jpeg pictures of the surface. The sample stage of the AFM can be controlled with either software in digitized steps of the size 2 μm or manually using a “tracking ball” mechanism. The sample stage also includes a vacuum hold-down system to lock samples in fixed position. The stage can accommodate samples and wafers of varying sizes up to a maximum of 200 mm in diameter, with a maximum field of scan of 90 μm^2 . For topography determination of a target, AFM using the height imaging in the tapping mode was employed. Samples were scanned at different surface regions with an average scan size of 10 $\mu\text{m} \times 10 \mu\text{m}$

and a scan rate of 0.800 Hz. The schematic diagram of the AFM used is shown in figure 3.7. The data scale was between 500.0 nm and 100.0 mV.

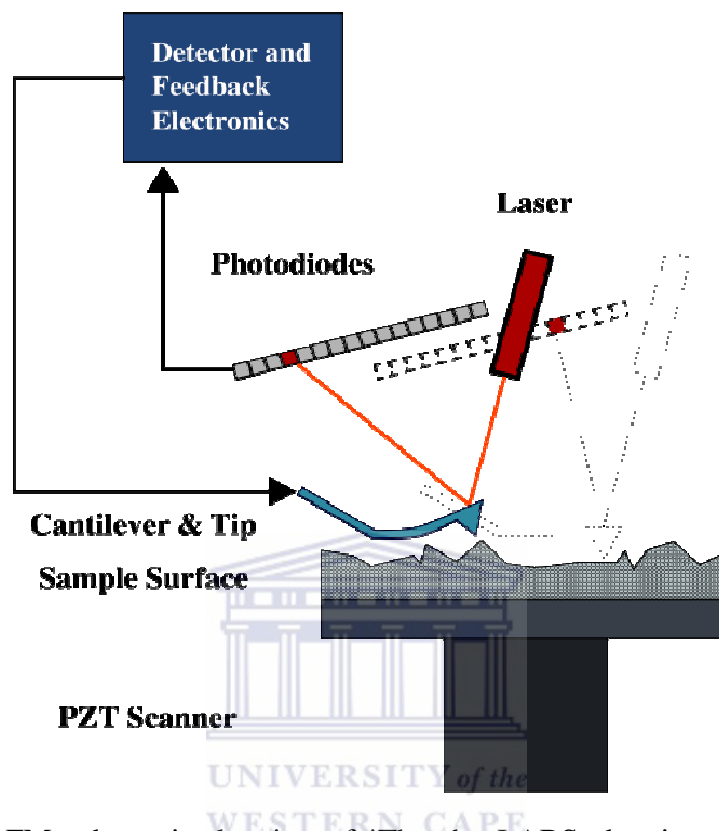


Figure 3.7: AFM schematic drawing of iThemba LABS showing sample surface, cantilever and tip, photodiodes, laser and detector.

3.2.4 X-ray diffraction analysis (XRD)

The crystal structure and orientation of targets were investigated by the x-ray diffraction method. Diffraction effects are observed when electromagnetic radiation impinges on periodic structures with geometrical variations on the length scale of the wavelength of the radiation. The interatomic distances in crystals and molecules amount to 0.15 - 0.4 nm which correspond in the electromagnetic spectrum with the wavelength of x-rays having photon energies between 3 and 8 keV. There are three different types of interaction in the relevant energy range. In the first, electrons may be liberated from their bound atomic states in the process of photoionisation. Since energy and momentum are transferred from the incoming radiation to the excited

electron, photoionisation falls into the group of inelastic scattering process. The second possible interaction process of inelastic scattering that the incoming x-ray beams may undergo is termed Compton scattering. Also in this process energy is transferred to an electron which proceeds without releasing the electron from the atom. Finally x-rays may be scattered elastically by electrons which is named Thomson scattering. The wavelength, λ of X-rays is conserved for Thomson scattering in contrast to the two inelastic scattering methods mentioned earlier on. It is the Thomson component in the scattering of X-rays is used in structural investigations by X-ray diffraction.

In laboratory X-ray tubes, electrons are accelerated onto an anode plate made from a specific metal of high purity. The electrons are emitted from the cathode filament and accelerated towards the anode plate under a high vacuum environment. The anode is typically fabricated from copper, chromium, molybdenum or another metal. The electron current between the filament and an anode may be adjusted by tuning the filament current in the range of some 10 mA. When impinging upon the anode the electrons are decelerated by their interaction with the target plate atoms leading to the emission of X-rays. The acceleration voltage in kV must be greater than the energy of the characteristic radiation required by the experiment in keV [Bir06][Dwo83]. Peaks in x-ray diffraction patterns are directly related to the atomic distances. The diffraction pattern is collected by varying the incidence angle of the incoming X-ray beam by θ and the scattering angle by 2θ while measuring the scattered intensity I (2θ) (figure 3.8). For a given set of lattice planes with inter planar distance of d , the condition of the diffraction peak can be written as a denotation below which is known as Bragg's law (equation 3.2), where n is an integer determined by the order of reflection.

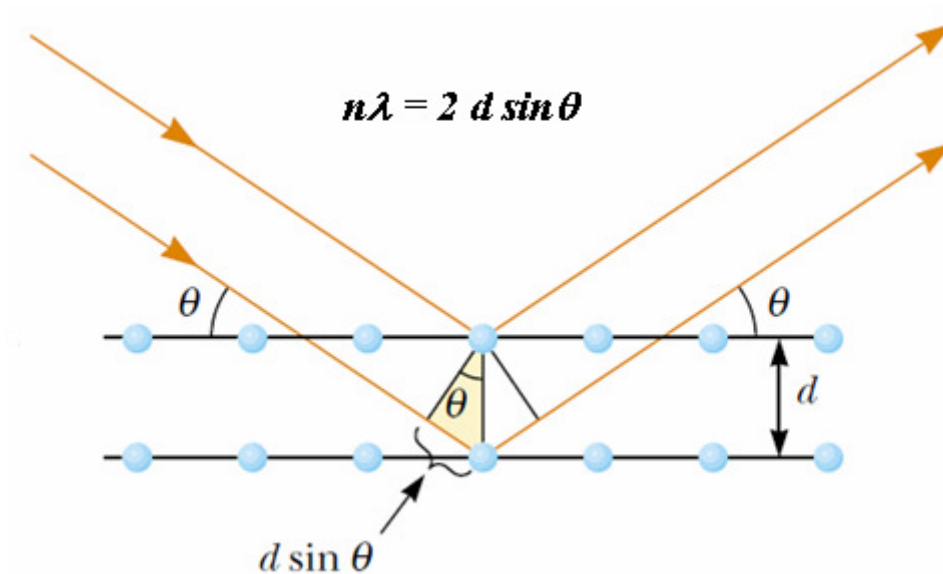


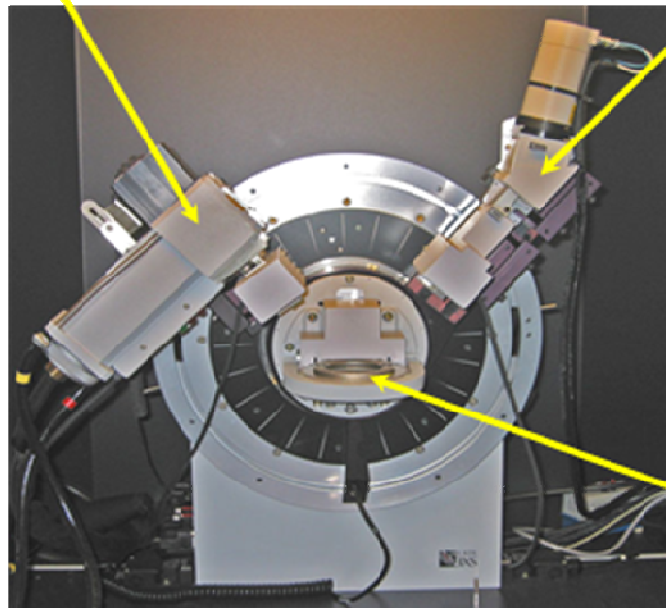
Figure 3.8: The schematic drawing of different sets of crystallographic planes that occur according to the Bragg's condition [Hun08].

$$n\lambda = 2d \sin \theta \quad (3.2)$$

Targets on aluminium frames were mounted on sample frame used on a D8 Advance Bruker X-ray diffractometer (see figure 3.9). Samples were analysed using a $\text{CuK}\alpha$ radiation with a wavelength of 1.5418 \AA . Angular steps were incremented by 0.05° and counts were collected for 0.5 seconds per step. The data was collected at 2θ from 25° to 85° angles. Two targets (3.6 and 12.8 mg.cm^{-2}) used in experiment were analysed before and after the experiment.

X-ray source

Detector



Sample

Figure 3.9: An image of D8 Advance Bruker X-ray diffractometer employed during the analysis of the targets.



3.2.5 Scanning electron microscopy (SEM)

Electron microscopes instruments uses a beam of highly energetic electrons to examine objects on a very fine scale. This examination can yield information about the topography (surface features of an object), morphology (shape and size making up an object), composition and crystallographic information. Electron microscopes were developed due to the limitations of microscopes, which are limited by the physics of light to 500x or 1000x magnification and a resolution of 0.2 μm [Vou08]. Several types of signals are produced from a surface in this process including backscattered, secondary and Auger electrons. Moreover X-ray fluorescence photons and other photons of various energies are also produced. All of these signals have been used for surface studies but the most commonly ones are the backscattered and secondary electrons which serve as basis of scanning electron microscopy.

When a sample is bombarded with electrons the highest counts region of the electron energy spectrum is due to secondary electrons. The secondary electron yield depends on many factors and is higher for high atomic number targets and at higher incidence angles. Secondary electrons are produced when an incident electron excites an electron in the sample and loses most of its energy in the process. The excited electron moves towards the surface of the sample undergoing elastic and inelastic collisions until it reaches the surface where it can escape if it still has sufficient energy [Wei69]. The backscattered electrons consist of high-energy electrons originating in the electron beam that are reflected or backscattered out of the specimen interaction volume. The production of backscattered electrons varies directly with specimen atomic number. This different production rates causes higher atomic number elements to appear brighter than lower atomic number elements. This interaction is utilised to differentiate parts of the specimen that have different average atomic number.

Scanning with SEM is accomplished by the two pairs of electromagnetic coils located within the objective lens. One pair deflects the beam in the x - direction across the sample and the other pair deflects it in the y - direction. Scanning is controlled by applying an electrical signal to one pair of scan coils, such that the electron beam strikes the sample to one side of the center axis of the lens system [Sko98]. By varying the electrical signal to this pair of coils (that is the x coils) as a function of time, the electron beam is moved in a straight line across the sample and then return to its original position. After completion of the line scan, the other set of coils (y coils in this case) are used to deflect the beam slightly, and the deflection of the beam using the x coils is repeated. Thus, by rapidly moving the beam the entire sample surface can be irradiated with the electron beam. The signals to the scan coils can be either an analog or digital signal. Digital scanning has an advantage that it offers very reproducible movement and location of the electron beam. The signal from the sample can be encoded and stored in digital form along with digital representations of the x and y positions of the beam.

Measurements for SEM were carried out on the ^{114}Cd target with a thickness of 12.80 mg.cm^{-2} since it was not prone to breakage under high vacuum during analyses because of its thickness. The samples were prepared by cutting them in a size that fits in the sample holder of the equipment. There were no further preparations needed on

the sample since cadmium is conductive. Samples were then glued to the substrate and placed to a substrate holder. The SEM analysis was conducted using the 40kV Hitachi X650 SEM equipped with EDAX energy dispersive spectrometer (EDS) and updated for full digitized imaging (see figure 3.10). Measurements were carried out at different magnifications from 25 x to 2000 x.

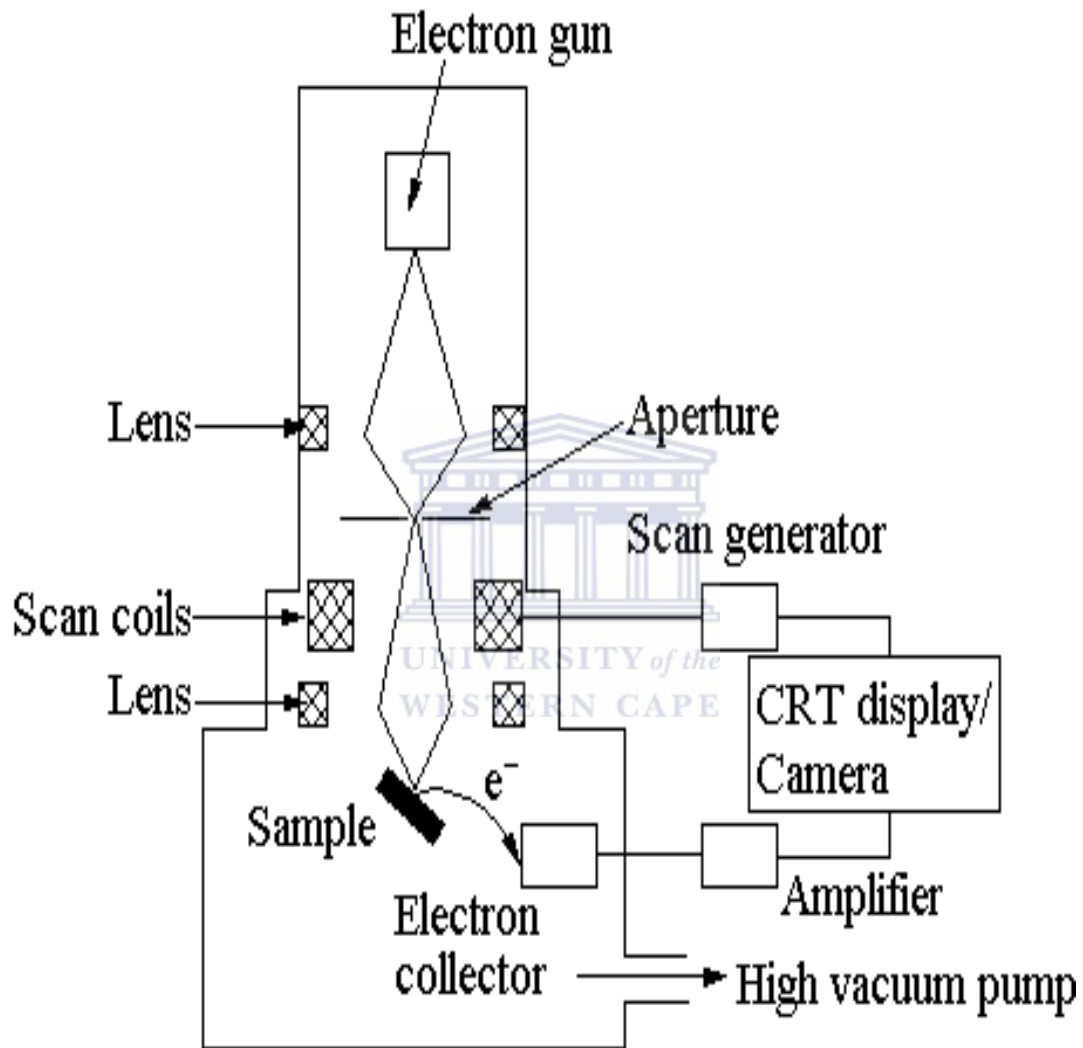


Figure 3.10: The schematic diagram showing general operational components of the SEM instrument used during the analysis of ^{114}Cd target at the University of Western Cape.

3.3 Conclusion

Six Targets were successfully manufactured by vacuum evaporation followed by mechanical rolling methods. Two targets were further characterised before and after their application in nuclear physics experiment for stopping power measurements. The thicknesses were measured directly by weight and area measurement to obtain density thickness. For stopping power experiment, a semi – thick target was needed which is considered as main target in this work. The stopping power experiment relied on the thickness of a semi-thick target and its purity. Therefore, thickness and elemental analyses of this target were quantitatively measured by RBS and PIXE. A second target used during the experiment, for a lifetime measurement was a 12.8 mg.cm^{-2} which is referred to as a thick target. Cadmium has a low melting point and nuclear physics experiments are conducted using high beam currents. Therefore crystal structure on both targets (3.6 and 12.8 mg.cm^{-2}) was studied before and after use in an experiment by XRD. This was done to investigate if there were any defects caused by beam of particles during the nuclear physics experiment. For surface characterisation of a semi – thick target, AFM and SEM were conducted on the target before and after the experiment. This was conducted to investigate any notable changes on the target that might have happened during the experiment. It should be noted that targets were not supposed to melt or evaporate throughout the experiment. Any evaporation occurred would have changed the thickness of a target and this would have affected stopping power measurements results [Lie09]. All the results obtained for the characterisations are discussed in chapter 4.

CHAPTER 4 RESULTS AND DISCUSSION

This chapter is divided into three sections. Section 4.1 gives results of the manufactured targets by vacuum deposition and rolling methods. Section 4.2 gives results obtained during the characterization of a semi-thick and thick targets measured by RBS, PIXE, XRD, AFM and SEM. The discussion of the results is in section 4.3.

4.1 Target manufacturing

Six targets were manufactured using a vacuum evaporation method followed by mechanically rolling and finally mounted on frames used on AFRODITE experiments as shown in figure 3.5. The targets on the frames and their thicknesses are listed in table 4.1. Targets thicknesses given in table 4.1 were determined after rolling process by mass and area measurement (equation 4.1). Targets were classified in thicknesses as thin ($0.5-1 \text{ mg.cm}^{-2}$), semi-thick ($3.6-3.9 \text{ mg.cm}^{-2}$) and thick (from $5 - 17 \text{ mg.cm}^{-2}$). It should be noted that the results of thin target are not included in the results since none were manufactured. From the table below only two targets with the following thicknesses were used in a stopping power experiment: 3.89 (semi-thick) and 17.1 mg.cm^{-2} (thick). Equation 4.1 below illustrates an example of how the thickness of the materials was calculated.

$$\text{Thickness}(\text{mg.cm}^{-2}) = \frac{\text{mass}(\text{mg})}{\text{Area}(\text{cm}^2)} = \frac{6.2}{1.58} = 3.89 \text{ mg.cm}^{-2} \quad (4.1)$$

Table 4.1: List of six ^{114}Cd targets, produced by vacuum evaporation as well as rolling techniques, and their thicknesses based on mass and area measurement.

Target Number	Target thickness (mg.cm^{-2})
1	3.89
2	8.3
3	10.2
4	11.9
5	12.8
6	17.1

4.2 Nuclear microprobe results

4.2.1 Thickness determination and quantification by RBS

Only one target was quantitatively analysed for thickness measurement using the RBS (Rutherford backscattering spectroscopy) technique. A particular interest was paid on a semi-thick target as the success of the stopping power measurement experiment was depending on it [Lie09]. The semi-thick target in this case had a thickness of 3.89 mg.cm^{-2} measured after the rolling process by mass and area measurement. The calculated optimal thickness using simulations programs, COMPA and GAMMA, was 3.65 to 3.9 mg.cm^{-2} and the thickness of the target was requested at this range. This thickness had to partially slow down the nuclei in a target before escaping to vacuum [Lie09]. The thickness value of the target was supposed to be determined accurately before use in the experiment. This is because mass/area method for the thickness determination only computes an average surface density.

Then, RBS thickness measurements were conducted for accurate determination of thickness. The thickness was measured after the experiment as well since cadmium has low melting point. This can lead to evaporation of the material since high currents are used during nuclear physics experiment. The RBS spectra of the backscattered protons are shown in figures 4.1 and 4.2. The RBS spectrum in figure 4.1 is for measurement before target bombardment with the silicon projectile during the experiment while in figure 4.2 the spectrum was obtained after the experiment. It should be noted that the measurements after the experiment were conducted on a beam spot on a target. The RBS spectra were analysed using a RUMP computer simulation package [Doo86]. Both spectra show a slope on the low energy side and a steep rise on the high energy side. Since homogeneity on the surface of the target was one of the requirements, therefore the variations of the target thickness were calculated using the fuzz option in RUMP computer package. The low energy slope corresponds to a layer with a thickness of 0.9 mg.cm^{-2} evaluated by fuzz option.

In both spectra, two small peaks are observed in the channels between 280 and 350 (energy 2.1 – 2.65 MeV). Although there were no thorough investigations conducted,

it was deduced that the two small peaks are those of carbon and oxygen. Thin films of cadmium tend to form oxygen layer on the surface and this was deduced by RBS analysis (see also figures 4.1 and 4.2). Carbon was also detected by RBS and this may result from the oil introduced by vacuum pumps from the evaporation system, see figure 3.1. There were no deviations in thickness results for the measurements conducted before and after the experiment. The overall thickness in both measurements performed by RBS technique was found to be $3.64 \pm 0.09 \text{ mg.cm}^{-2}$ for various scanned target surface regions.

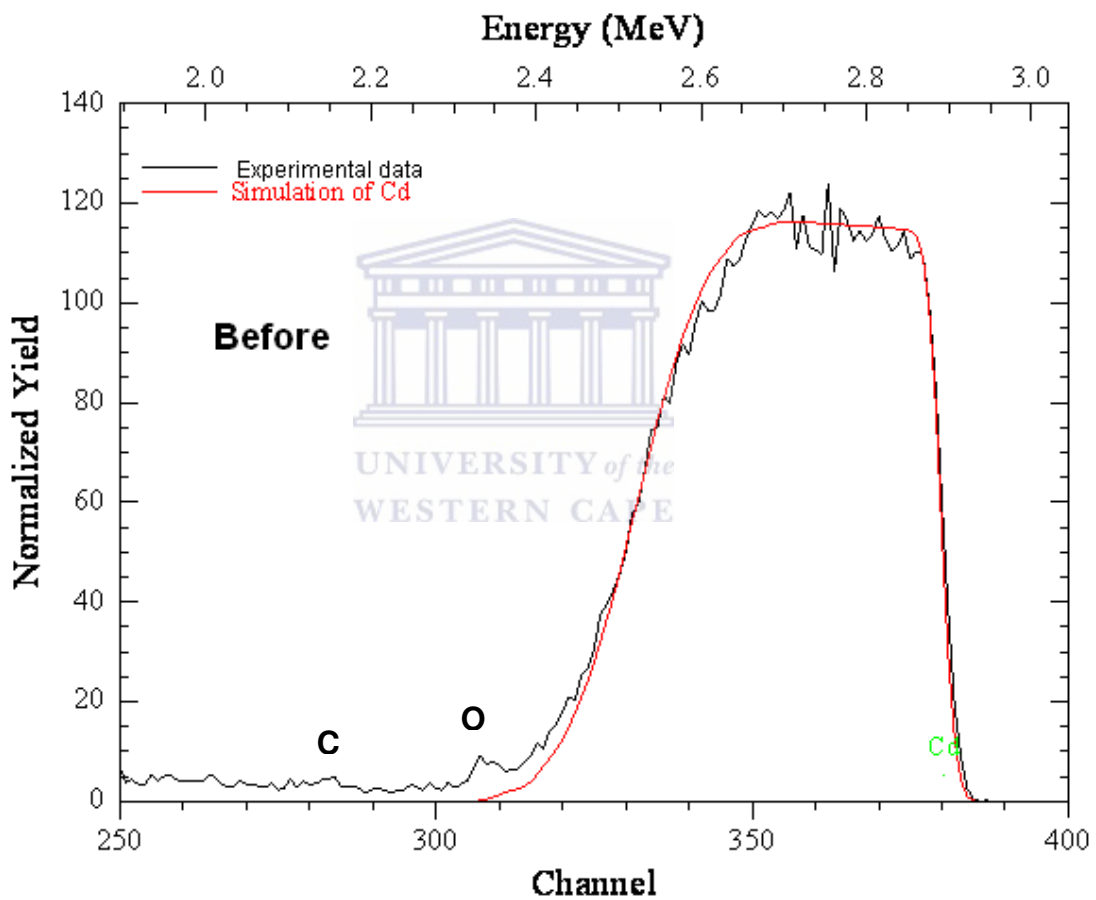


Figure 4.1: The RBS spectrum of ^{114}Cd target before being irradiated with ^{28}Si projectile.

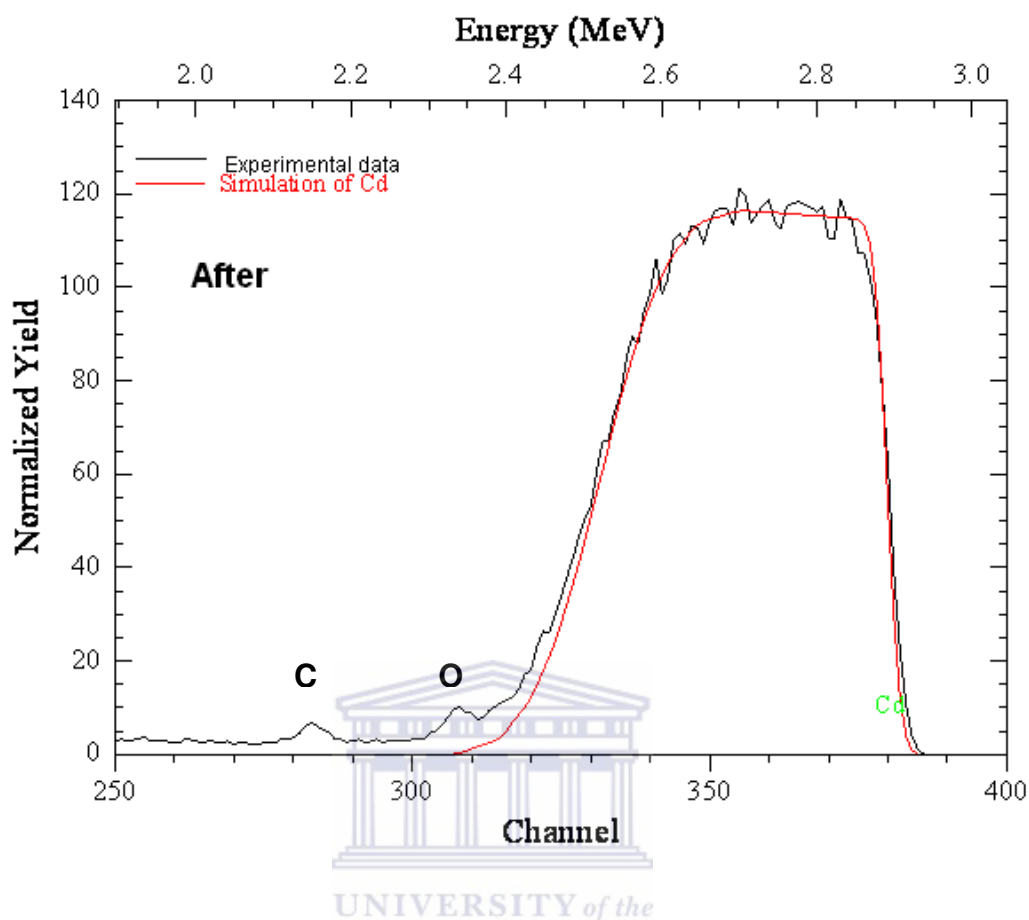


Figure 4.2: RBS spectrum of ^{114}Cd obtained on the beam spot resulted after the experiment.

4.2.2 Elemental distribution analysis of by PIXE

It was indicated earlier that nuclear targets should be free from external contaminants as these will bring changes to the density and stopping power of the target material [Mun88]. Particle Induced X-ray Emission (PIXE) analysis was conducted on the manufactured semi-thick target ($3.6 \text{ mg}\cdot\text{cm}^{-2}$) for elemental distribution of ^{114}Cd and trace impurities in a target. The analyses were conducted before the experiment as only the purity of the target had to be known before use in the experiment. The mapping and the trace impurities of the ^{114}Cd were taken using the L and K lines as presented in figure 4.3(a) and (b), respectively. Elemental maps exhibiting two dimensional distribution patterns of the metal were generated using the dynamic analysis developed by Ryan [Rya01] and Prozesky *et.al* [Pro95]. Elemental mapping

image in figure 4.3(a) shows an even distribution of cadmium elements which is the indication of homogeneity. On the image in figure 4.3(b), the yellow colour (Cd) is more dominant than blue which indicates some contamination in trace amounts. The contamination was found to be iron (Fe) which might have come from the rolling plates.

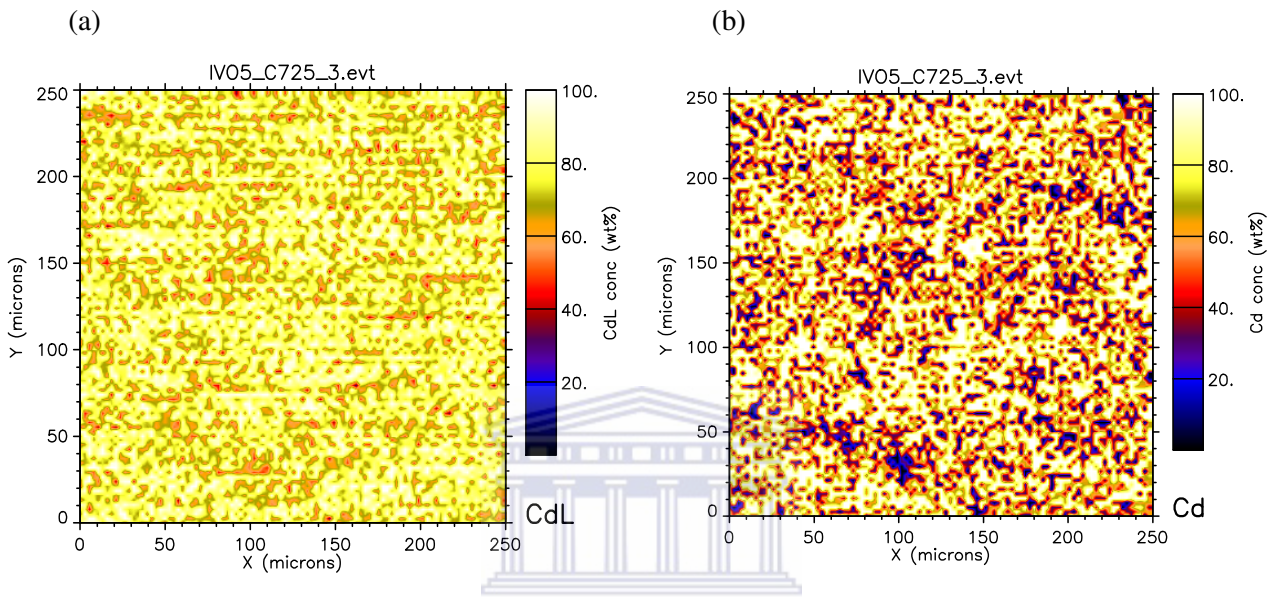


Figure 4.3: The contour maps of $3.6 \text{ mg}\cdot\text{cm}^{-2}$ obtained using the (a) L lines and (b) K lines during PIXE analysis.

In both mappings the results showed that the elemental distribution in a target was 90 % Cd with some traces of iron as the contaminant. It should be noted also that the isotopically enrichment of the target material was 90.01% (in ^{114}Cd material) and the rest of the trace amounts were other nuclides.

4.2.3 Phase analysis by X – ray diffraction (XRD)

A crystal structure of the manufactured targets were investigated by XRD in order to observe if there was any change on the crystal structure after targets were irradiated during the experiment. It should be noted that the melting point of Cd is 321°C and this is relatively low for nuclear physics experiments as they are conducted using high energy beam currents. The probabilities of beam damage on targets with low melting points are highly possible. Targets can melt or have disoriented crystal structures due

to the high currents used [Mun88]. For the success of the experiment where Cd targets were used [Lie09], targets are not supposed to melt as the thickness of the targets is required to remain constant for the duration of the experiment. Figure 4.4 shows the hexagonal crystal structure and the orientations of ^{114}Cd targets with 3.6 and 12.8 $\text{mg}\cdot\text{cm}^{-2}$ thicknesses. The analyses were conducted before target exposure to particle beam and after the experiment. The XRD results (see figure 4.4) show no defects in the structure of the irradiated targets since they show the same Cd orientations as the unirradiated targets. The vertical axis records X-ray intensity whereas the horizontal axis records angles in degrees 2-theta. Results of all targets shows no differences in orientation on both targets before and after the experiment. The colour coded spectra are shown in figure 4.4.

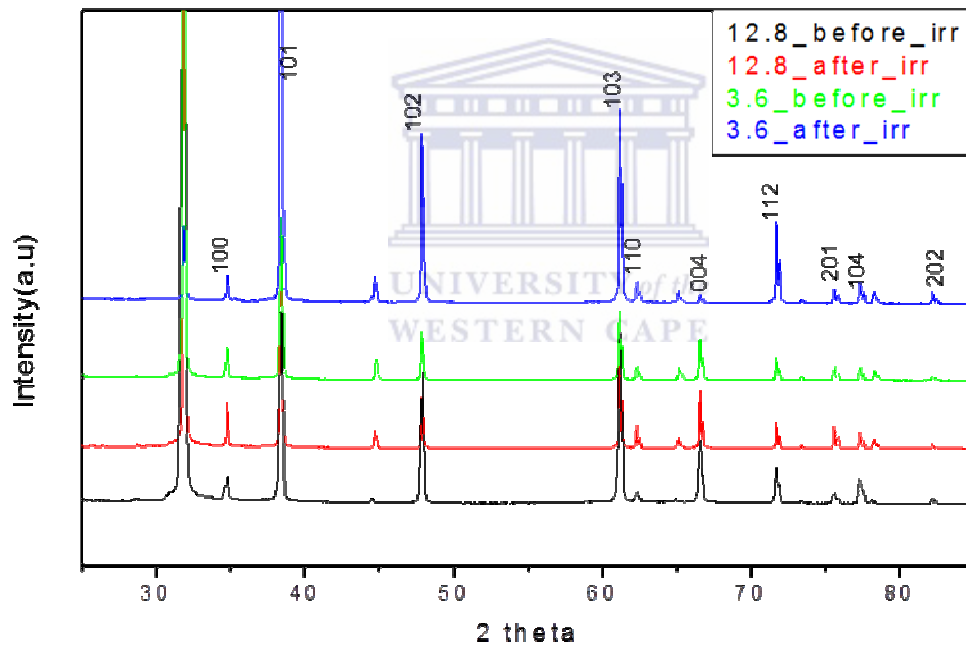


Figure 4.4: The XRD spectra of two ^{114}Cd targets.

4.2.4 Surface topography and morphology characterisation

4.2.4.1 Atomic force microscopy (AFM)

The topography of the target was investigated by AFM before and after irradiation with the ^{28}Si beam. Snapshots were taken using two and three dimension modes in which the later was for a better view on the topography. This analysis was performed in order to obtain information regarding the surface homogeneity of a target by measuring the roughness (deviation of maximum peaks from minimum peaks). For the stopping power experiment using the semi-thick target method, homogeneity of a target was one of the requirements [Lie09]. AFM images were taken on a 3.6 mg.cm^{-2} target (semi-thick), and three dimensional images are shown in figure 4.5.

The AFM images were taken in surface areas of ($20 \mu\text{m} \times 20 \mu\text{m}$) and ($10\mu\text{m} \times 10 \mu\text{m}$) on unirradiated targets. The average roughness was found to be 42.6 nm and 21.5 nm and it decreased by a factor of two for the later as shown in figure 4.5(a) When the roughness was measured on the beam spot caused by irradiation the roughness increased to 66.7 nm (the image is shown in figure 4.5 (b)). This increase might be due to sputtering of the target during irradiation with a beam. The target material did not evaporate/melt as this would have been confirmed by RBS during the thickness measurement.

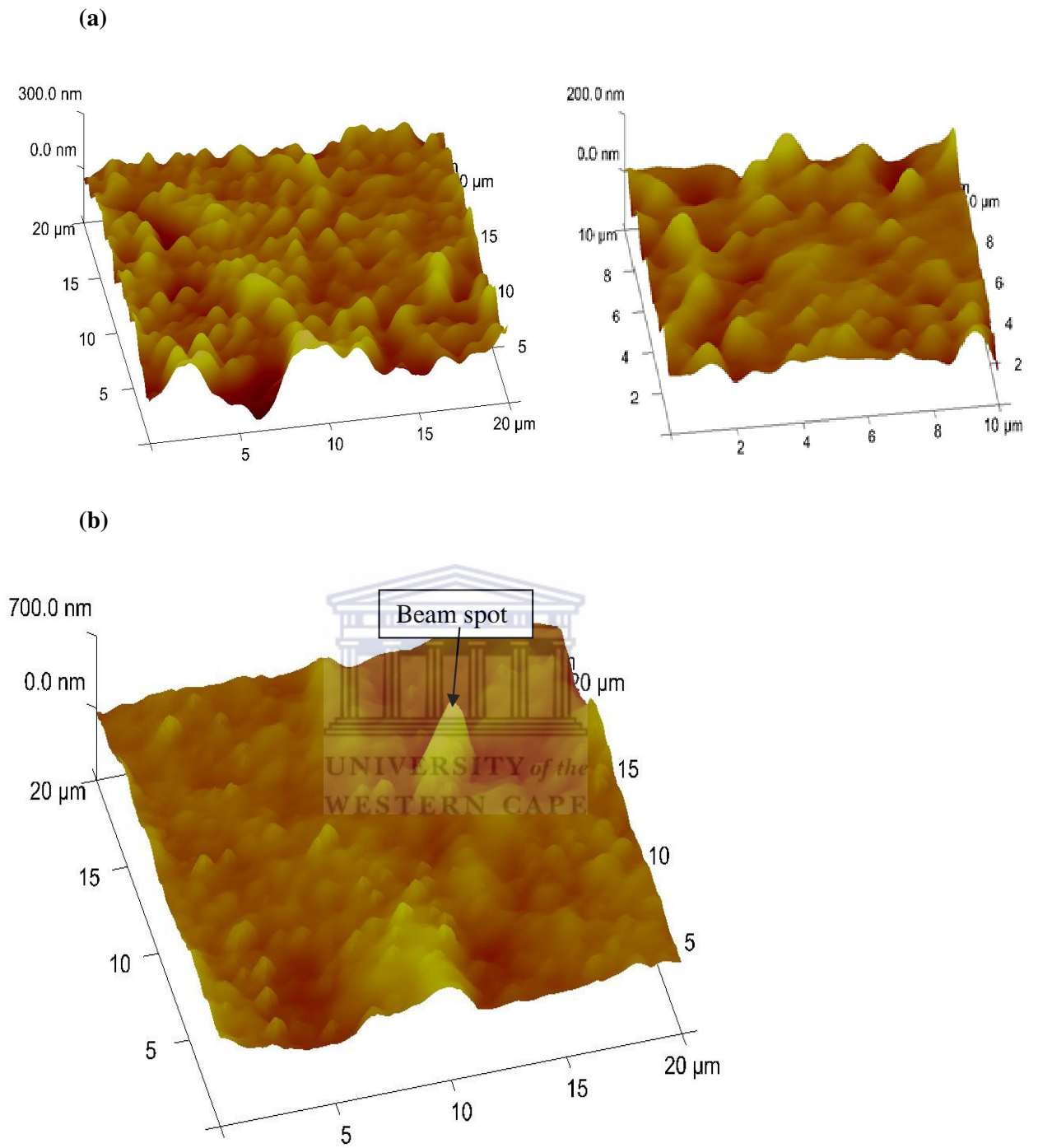


Figure 4.5: (a) AFM images representing a three dimensional images of unirradiated 3.6 mg. cm^{-2} target taken using different surface areas and (b) A three dimensional AFM image taken on beam spot of a $3.6 \text{ mg.cm}^{-2} \text{ }^{114}\text{Cd}$ target.

4.2.4.2 Scanning electron microscopy (SEM)

The scanning electron microscopy was used to determine if there were any defects on the surface caused by a ^{28}Si beam on the ^{114}Cd target. This analysis was only conducted on the thick target. This target was chosen since the semi-thick target was not thick enough to withstand the high vacuum in SEM chamber. Furthermore, the analysis was performed for surface topography information of the target. The final step in target manufacturing uses the rolling method which may cause surface unevenness that may be the result of the defects on the mills of the rolling mill. SEM was performed on the unirradiated surfaces and the beam spot for comparison. SEM images are shown in figures 4.6 – 4.8. Figure 4.6 show the images taken on a beam spot and on unirradiated surface of the target. The image presents the smooth surface with some defects due the manufacturing process (scratch).

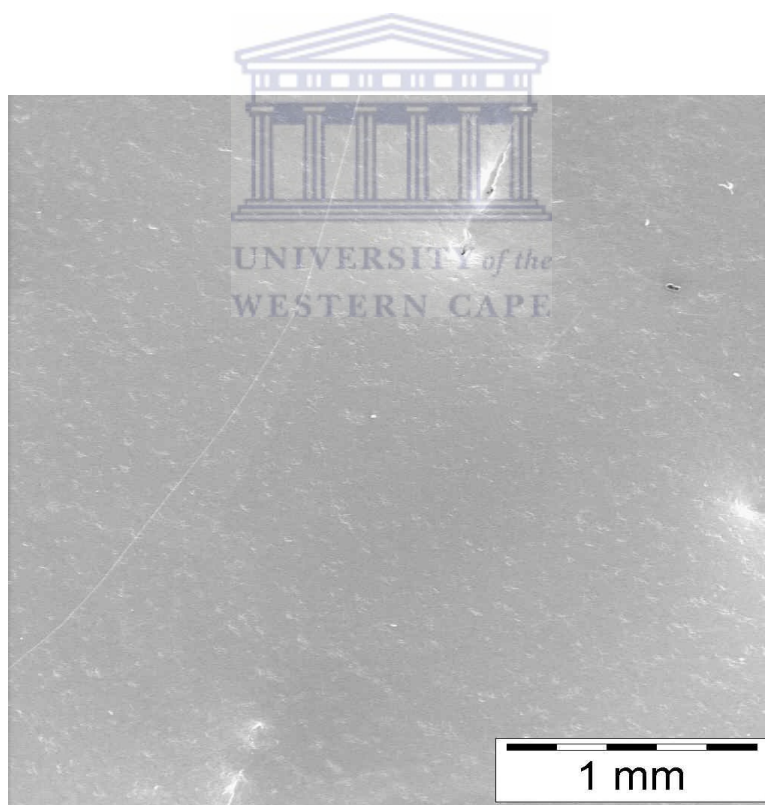


Figure 4.6: Surface morphology obtained by SEM of a $12.6 \text{ mg.cm}^{-2} \text{ }^{114}\text{Cd}$ target using a 35x magnification.

The surface morphologies presented in figure 4.7 shows uneven surfaces on the target when different magnification ranges were used. The surface is seen with a swollen

crust and this was observed in all images. This might be due to dirt present on the surface of the target that occurred during the rolling process. This effect could have been introduced by the rolling plates or dust. The images on the beam spot don't show any significant damage caused by the beam on the target. In addition, Scanning Electron Microscopy results revealed unevenness on some areas of the target surface in a form of a swollen crust. External dirt appeared on the target surface, shown in SEM images (figures 4.7-4.8). There were no voids or cracks observed as this would be a disadvantage for life time measurements which would affect the accuracy of the experimental results [Gal70]. In addition images in figure 4.8 also show dirt present (the long diagonal object) on the target surface and crust on the surface is also observed.

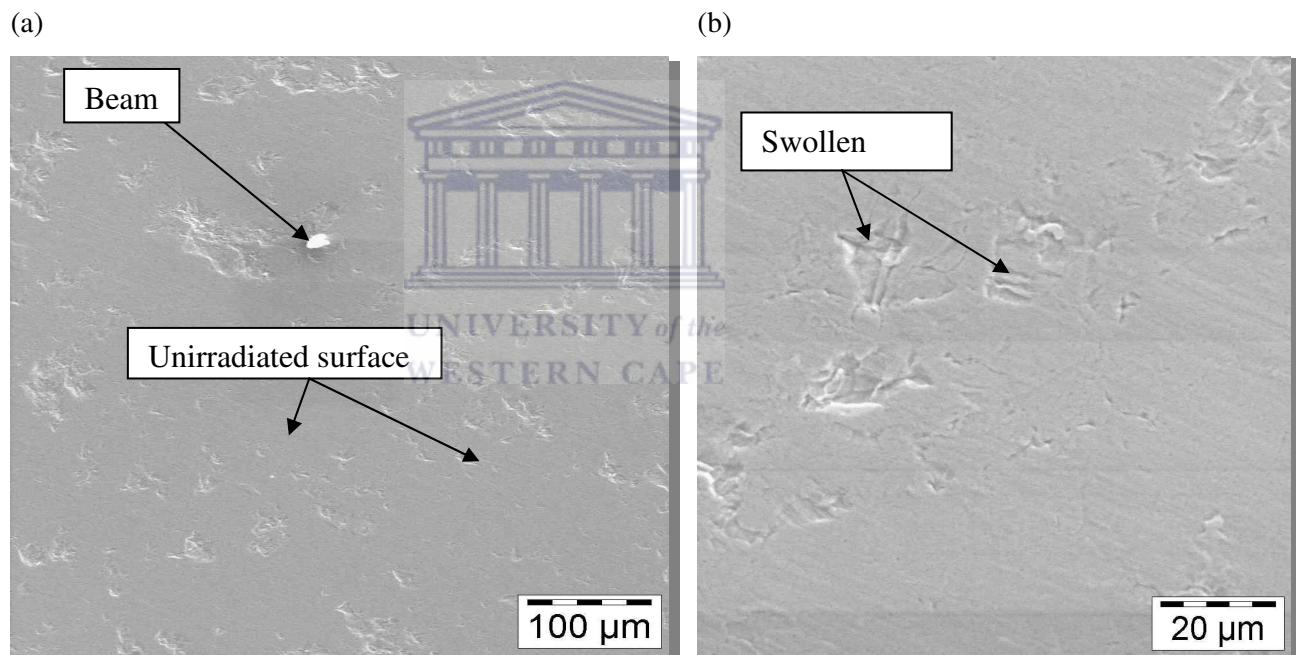


Figure 4.7: SEM images of ^{114}Cd target with a thickness of $12.6 \text{ mg}\cdot\text{cm}^{-2}$ obtained using lower (a) and (b) higher magnification.

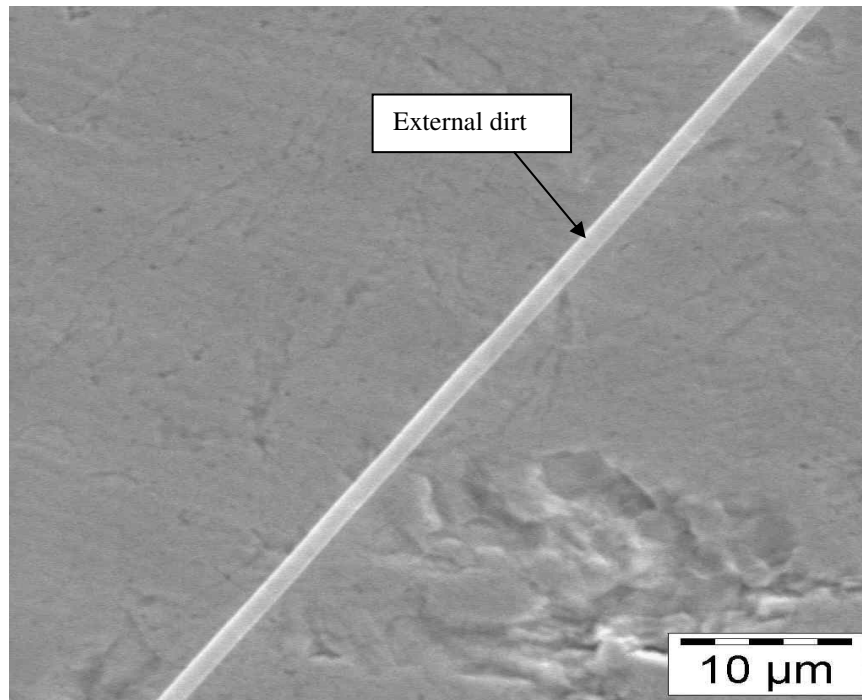


Figure 4.8: SEM images of ^{114}Cd illustrating external dirt from the target surface taken at higher magnification.

4.3 Conclusion



Targets of various thicknesses were manufactured by vacuum deposition and rolling methods. They were further characterised for thickness determination. Thickness results obtained using RBS were compared to those obtained by mass and area measurement. Thicknesses of $3.9 \text{ mg}\cdot\text{cm}^{-2}$ (for mass and area shown in table 1) and $3.6 \text{ mg}\cdot\text{cm}^{-2}$ from Rutherford backscattering (RBS) measurements were obtained. This thickness was required to stop the nuclides of interest in a target before releasing them to vacuum. Such comparison showed a 30% percentage difference. The difference is due to: RBS measurements are conducted on a specific spot whereas weight area measurement is the average of the entire surface area. However, both results meet the thickness range for a semi-thick target for a life-time measurement [Lie09]. In addition to RBS and PIXE, XRD analysis was used for crystal structure investigation of the targets. This was performed in order to observe if there were any defects occurring on the crystal structure of the targets after the experiment. The XRD results (see figure 4.4) show no defects in the structure of the irradiated target since

they show the same Cd orientations as the unirradiated targets. This confirms that there was no melting occurred on both targets caused by high energy beam currents.

The topography analysis performed on a semi-thick target by Atomic Force Microscopy (figure 4.5) showed a smooth surface with an average calculated roughness of 42.6 nm and 21.5 nm. The roughness on the target increased to 66.7 nm when the analysis was performed on the beam spot after irradiation. Both results obtained on AFM and SEM analysis revealed some unevenness on some areas of the target surface. Nevertheless, there were no voids or cracks observed on SEM images as this would be a disadvantage for the life time measurement which would affect the accuracy of the experimental results [Gal70]. All in all, targets produced met all the requirements for the stopping power experiment and they were used successfully in an experiment which yielded useful results for the nuclear physics research community [Lie09].



CHAPTER 5 SUMMARY

Cadmium targets of different thicknesses were synthesised and characterised by complementary methods. Results obtained from this show that:

- Targets that were produced presented a homogeneous surface in terms of thickness, more especially on the area of interest of a target where the bombardment with the beam of particles was carried out.
- Semi-thick (3.6 mg.cm^{-2}) target remained unchanged which is a good sign for a stopping power experiment, although some other parts of target material show increased roughness after the experiment.
- Characterisation results showed no radiation damage occurred in target during the experiment otherwise if it happened it would indicate that the experiment failed.
- Target material did not contain any competing nuclides with the nuclides of interest which is the sign of purity.
- Targets had minor defects on the surface introduced by the manufacturing methods.
- Dirt and the condition of the equipment normally affect the quality of targets. Crust as observed on the target surface and this may be the result of the unevenness of the rolling mills surface.

Recommendations

- Targets need to be stored under vacuum in order to prevent the formation of an oxide layer on the thin layer of Cd metal.
- Oil free pumps are recommended for vacuum system to avoid contamination
- Rolling mills with defective rolling surfaces introduce defects on the rolled materials, mills need to be changed or surface be smoothed regularly.

REFERENCES

- [Abd07] A. M. Abdelkader and E. El-Kashif, ISIJ International, 47, No.1, (2007) 25-31.
- [Ada78] H. L. Adair, Report LBL-7950 (1978) 1.
- [Ang84] J. C. Angus, J. E. Stultz, P. J. Shiller, J. R. Macdonald, M. J. Mirtich, S. Domitz, Thin Solid Films, 118 (1984) 311-320.
- [Bau79] H. Baumann and H.L. Wirth, Nuclear Instruments and Methods, 167 (1979) 71-72.
- [Bir06] M. Birkholz, Wiley-VCH Verlag, ISBN 3-527-31052-5, 2006.
- [Bir08] D. Biro, P. B. Barna, L. Szekeley, O. Geszsti, T. Hattori, A. Devenyi, Nuclear Instruments And Methods, A590 (2008) 99-106.
- [Bor00] V. D. Borisevich, H. G. Wood, Academic Press, 111 (2000) 3202-3207.
- [Cec88] A. Cecchi, Newsletter No.14, 2 (1988) 10.
- [Chi71] W. A. Childs, G. H. Lenz, Nuclear Instruments and Methods, 95 (1971) 441-443.
- [Dio91] J. S. Dionisio, Z. Meliani, C. Schuck and Ch. Vieu, Nuclear Instruments and Methods in physics, A303 (1991) 9-18.
- [Dol93] G. Dollinger, M. Boulouednine, T. Faestermann, P. Maier-Komor, Nuclear Instruments and Methods, A334 (1993) 187-190.
- [Doo86] L. R. Doolittle, Nuclear Instruments And Methods, B15 (1986) 227.
- [Dwo83] S. Dworkin, J. Math, Phys. 34, Vol. 7 (1983) 2965.
- [Ebe04] K. Eberhardt, M. Schadel, E. Schimpf, P. Thorle, N. Trautmann, Nuclear Instruments and Methods, A521 (2004) 208-213.
- [Fan08] Q. Fan and G. Xu, Nuclear Instruments and methods in Physics Research, A 590 (2008) 91-95.
- [Fei93] R. M. Feinberg and R.S. Hargrove, Overview of Uranium Atomic Vapor Laser Isotope Separation, August 1993.
- [Fle95] R. Flemming, RBS Theory, [www.cea.com/cai/rbstheo/inro.html\(1995\)](http://www.cea.com/cai/rbstheo/inro.html(1995))
- [For83a] J. L. C. Ford, Proceedings of International nuclear target development society (1983) 45-88.

- [For83b] J. L. C. Ford, Proceedings of workshop of the International Target Development Society, (1983) 45-65.
- [Gal04] Galloway Group, A Guide to understand and Using The AFM, Spring 2004.
- [Gal70] J. L. Gallant, Nuclear Instruments and Methods, 81 (1970) 27-28.
- [Gal83] J. L. Gallant, P. Dmytrenko, Proceedings of the Nuclear Target Development Society (1983) 219-222.
- [Glo65] K. M. Glover, P. S. Robinson, Report AERE-R 5097 (1965) 50.
- [Glo72] K. M. Glover, F. J. G. Roggers and T. A. Tuplin, Nuclear Instruments and Methods, 102 (1972) 443-450.
- [Gro99] M. P. Groover, Fundamentals of Modern Manufacturing, New York, 1999.
- [Hea72] J. M. Heagney and J. S. Heagney, Nuclear Instruments and Methods, 102 (1972) 451-455.
- [Hel00] A. Heller, Laser Technology Following in Lawrence's Footsteps, (2000) 13.
- [Hin72] A. G. Hins, Nuclear Instruments and Methods, 102 (1972) 425-430.
- [Hun08] M. R. C. Hunt, Physical Review, B78 (2008) 153408.
- [Jan83] R. V. F. Janssens, Proceedings of workshop of the International Target Development Society, (1983) 119-136.
- [Kar72] F. J. Karasek, Nuclear Instruments And Methods, 102 (1972) 457-458.
- [Kat69] S. Kato. Nuclear Instruments and Methods, 75 (1969) 293-296.
- [Kaz05] M. Kazeminezhad, A. K. TAheri, Journal Processing, 160 (2005) 313-320.
- [Khe08] N. Y. Kheswa, E. Z. Buthelezi and J. J. Lawrie, Nuclear Instruments and Methods, A590 (2008) 114-117.
- [Kob82] E. H. Kobisk, H.L. Adair, Proceedings of the 11th World Conference of the International Target Development Society, (1982) 28-57.
- [Kue72] P. R. Kuehn, F. R. O'Donnell and E. H. Kobisk, Nuclear Instruments and Methods, 102 (1972) 403-407.
- [Kwi79] J. Kwinta, H. Folger, Nuclear Instruments and Methods, 167 (1979) 65-70.
- [Lan87] R. G. Lanier, UCRL-95543, (1987) 1-6.

- [Lie08] D. Liebe, K. Eberhard, W. Hartmann, T. Hager, A. Hubner, J. V. Kratz, Nuclear Instruments and methods in Physics Research A 590 (2008) 145-150.
- [Lie09] E. O. Lieder, A. A. Pasternak, R. M. Lieder, R. A. Bark, E. A. Lawrie, J. J. Lawrie, S. M. Mullins, S. Murray, S.S. Ntshangase, P. Papka, N. Kheswa, W.J. Przybylowicz, P.T. Sechogela and K.O. Zell, Nuclear Instruments and methods in physics research, A607 (2009) 591-599.
- [Lor89] P. Lorenzen, H. Rothard, K. Kroneberger, J. Kemmler, M. Burkhard, K.O. Groeneveld, Nuclear Instruments and Methods, A282 (1989) 213-216.
- [Mag82] J. C. Magiore, Los Alamos Science, Summer, (1982) 27-45.
- [Mai81] H. J. Maier, IEEE Transactions on Nuclear Science, Vol. NS – 28, No. 2, (1981) 1576.
- [Mai89a] H. J. Maier, in Physics Research, A282 (1989) 113-115.
- [Mai89b] H. J. Maier, H. U. Friebel, D. Frischke and R. Grossmann, Nuclear Instruments and Methods in physics Research, A282 (1989) 128-132.
- [Mai91a] H. J. Maier, Nuclear Instruments and Methods in Physics Research, A303 (1991) 172-181.
- [Mai91b] P. Maier-Komor and G. Dollinger, Nuclear Instruments and Methods in Physics Research, A303 (1991) 168-171.
- [Mai91c] P. Maier-Komor, Nuclear Instruments and Methods, B56/57 (1991) 921.
- [Mai93] S.A. Maierov, A.N. Tkachev and S.I. Yakovlenko, Laser Physics, Vol.4 No.3 (1994) 624-630.
- [Mee93] A. Meens, I. Rossini, J.C. Senns, Nuclear Instruments and Methods, A334 (1993) 200-202.
- [Msi06] M. Msimanga, M. Mc Pherscon, Material Science and Engineering, B127 (2006) 47-54.
- [Mun88] G. Munzenberg, F. P. Hessberger, W. Faust, H. Folger, S. Hofmann, K. H. Schmidt, H. J. Schott, P. Armbruster, Nuclear Instruments and Methods in physics, A282 (1988) 28-35.
- [Pal93] J. Pal. D. Kabira, J. D. R. Avasth, Nuclear Instruments and Methods, A334 (1993) 196-199.

- [Pro95] V. M. Prozesky, W. J. Przybylowicz, E. van Achterbergh, C.L. Churms, C.A. Pineda, K. Springhorn, J.V. Pilcher, C.G. Ryan, J.H. Kritzinger, T. Schmitt, Nuclear Instruments And Methods, B104 (1995) 36.
- [Smi11] R.Smith www.y12.doe.gov/library/pdf/about/history/info_materials/05-0181.pdf
- [Rou10] D. Rousseau and J. Lepingwell, International Atomic Energy Agency Symposium 2010, IAEA-CN-184/262.
- [Rya01] C. G. Ryan, Nuclear Instruments And Methods, B181 (2001) 170.
- [Sca75] Scaife, P.R. Hanley and K.H. Purser, Proceedings of the 4th Annual Conference of the INTDS, ANL/PHY/MSD-76-1 (1975) 75.
- [Sch98] D .K. Schroder, Semiconductor Material and Device Characterisation, 2nd Ed, Wiley, New York, 1998.
- [Sed72] W.A. Sedlacek, Nuclear Instruments and Methods, 102 (1972) 429-431.
- [Set09] F. Settle, Nuclear Chemistry Uranium Enrichment, 2005 -2009.
- [Sin83] A. Singh. and C. S Harendranath, Journal of Material Science, 18 (1983) 3606-3610.
- [Sko98] D. A. Skoog. F. J. Holler and T.A. Nieman, Principles of Instrumental Analysis, 5th Ed, (1998) 535-561.
- [Sle72] G. Sletten and P. Knudsen, Nuclear Instruments and Methods, 102 (1972) 459-463.
- [Sto97] A. Stolarz, Nuclear Instruments and Methods in Physics Research, A397 (1997) 114-116.
- [Suz70] T. Suzuki, Nuclear Instruments and Methods, 87 (1970) 311-312
- [Tak07] T. Takamiya, T. Ohtsuki, H. Yuki, T. Mitsugashira, N. Sato, T. Suzuki, M. Fujita, T. Shinozuka, Y. Kasamatsu, H. Kikunaga, A. Shinohara, S. Shibata, T.Nakanishi, Applied Radiation and Isotopes, 65 (2007)32-35.
- [The79] The Great Soviet Encyclopedia, 3rd Edition (1970-1979).
- [Uet97] N. Ueta, W.G.P. Engle, N.H. Medina, D. Perira, L.C. Chamon, Nuclear Instruments and Methods in Physics Research, A397 (1997) 163.
- [Ver72] V. Verdingh, Nuclear Instruments and Methods, 102 (1972) 431-434.
- [Vou08] B. Voutou, E.C. Stefanaki, Physics of Advanced Materials, Winter School, 2008.

- [Wal62] G. K. Walters, L. D. Schearer, F. D. Colegrove, *Physical Review Letter*, 59 (1962) 502-505.
- [Wat03] D. A. Waters, SPLG Workshop, 2003.
- [Wei69] R. M. Weinbrandt, I. Fatt, *Rock Mechanics- Theory and Practice Proceedings of the 11th Symposium on Rock Mechanics Berkeley, CA, June 16-19, (1969) 629-641.*
- [Wiki] en.wikipedia.org/wiki/Gas_Centrifuge
- [Woo84] D. P. Woodruff and T.A. Delchar, T.A (1994), *Modern Techniques of Surface Science*, 2nd Ed, Cambridge University Press, Cambridge.
- [Yaf62] L. Yaffe, *Annual Review of Nuclear Science*, Vol. 12, (December 1962), 153-188.

